UCRL-11575

University of California

Ernest O. Lawrence Radiation Laboratory

TWO-WEEK LOAN COPY

This is a Library Circulating Copy which may be borrowed for two weeks. For a personal retention copy, call Tech. Info. Division, Ext. 5545

VAPOR PRESSURE DETERMINATION OF MANGANESE ACTIVITIES IN IRON-MANGANESE ALLOYS

Berkeley, California

DISCLAIMER

This document was prepared as an account of work sponsored by the United States Government. While this document is believed to contain correct information, neither the United States Government nor any agency thereof, nor the Regents of the University of California, nor any of their employees, makes any warranty, express or implied, or assumes any legal responsibility for the accuracy, completeness, or usefulness of any information, apparatus, product, or process disclosed, or represents that its use would not infringe privately owned rights. Reference herein to any specific commercial product, process, or service by its trade name, trademark, manufacturer, or otherwise, does not necessarily constitute or imply its endorsement, recommendation, or favoring by the United States Government or any agency thereof, or the Regents of the University of California. The views and opinions of authors expressed herein do not necessarily state or reflect those of the United States Government or any agency thereof or the Regents of the University of California.

Special thesis UCRL-11575

UNIVERSITY OF CALIFORNIA
Lawrence Radiation Laboratory
Berkeley, California

AEC Contract No. W-7405-eng-48

VAPOR PRESSURE DETERMINATION OF MANGANESE ACTIVITIES IN IRON-MANGANESE ALLOYS

Prodyot Roy

(Ph. D. Thesis)

August 1964

Reproduced by the Technical Information Division
directly from author's copy.

Vapor Pressure Determination of Manganese Activities in Iron-Manganese Alloys

Prodyot Roy, Inorganic Materials Research Division, Lawrence Radiation Laboratory, and Department of Mineral Technology, College of Engineering, University of California, Berkeley, California.

TABLE OF CONTENTS

	Page
Introduction	1
Knudsen Effusion Method	6
Torsion Effusion Method	8
Thermodynamics	12
The Apparatus	15
Furnace Assembly	15
Suspension System	18
Materials	25
Method of Analyses	25
Composition of the Alloys	27
Experimental Procedure	28
Knudsen Effusion Method	28
Torsion Effusion Method	30
Experimental Results	40
Discussion	46
Electron Probe Analyses	48
Kinetics of Evaporation Process	48
Interpretation of the Data	53
Conclusion	57
Acknowledgements	58
Tables	59
References	82
Appendix	84

I. INTRODUCTION

The study of the thermodynamics of alloys should ultimately lead to a general theory of the behavior of metallic atoms in the environment of alloy phases. From such a theory it might be possible to deduce the structures and properties of alloy systems from the properties of their component elements.

Very little thermodynamic data are available for high melting transition metal alloys, although they are technologically the most important class of alloys. The lack of investigation is due to difficult experimental problems associated with thermodynamic measurements at high temperatures. Solution calorimetry using liquid metal solvents is not very accurate at the high temperatures necessary to dissolve transition metals. Equilibrium measurements to determine activities involve several problems which will be discussed in detail.

The object of this investigation was to determine the Gibbs energies, heats, and entropies of formation of face-centered-cubic gamma-phase iron-manganese alloys at high temperatures. This might be done by electromotive force measurements of suitable cells or by measurements of equilibrium vapor pressures of manganese over the alloys and over pure manganese. The advantages and disadvantages of these methods are discussed in the following pages. For the present work the methods chosen were Knudsen and torsion effusion measurements of vapor pressures.

Application of these dynamic methods to alloy phases of variable composition involves a novel problem which has not been thoroughly investigated. During vaporization the surface concentration of the more volatile component becomes depleted; it may be replaced by diffusion from the interior of the sample. Only if diffusion is rapid compared with vaporization are equilibrium values obtained. In this work the effects of depletion have been more closely examined than before, with the result that large corrections were found necessary to the data found in the literature for the iron-manganese alloys low in manganese content.

In the emf technique the relative partial molar Gibbs energy of component B, $\Delta\bar{G}_B$, is determined from the measured potential as $\Delta\bar{G}_B = -n\,\mathcal{F}\,E_B$, where E_B is the voltage between an electrode composed of pure B and one composed of the alloy $A_{1-x}B_x$ and $\mathcal{F}$ is the Faraday constant. The electrolyte, which may be solid or liquid, contains B ions with charge B^{+n}. In order to operate the cell successfully the following conditions must be obtained:

(a) The conduction must be completely ionic.

(b) The rate of diffusion from the interior must be sufficient to maintain the equilibrium concentration at the surface of the alloy.

(c) Side reactions must not occur between electrode and electrolyte. Normally the two elements must differ considerably in electropositivity.

(d) The conducting ions must have a unique valence.

Although theoretically equilibrium emf measurements have several advantages over dynamic measurements, it is very difficult to obtain a suitable electrolyte which satisfies the above conditions. However, in recent years several successful attempts have been made using solid electrolytes at high temperatures. This technique could develop into a useful method for measuring the thermodynamic properties of high melting alloys.

Vapor pressure measurements may be direct or indirect. In a closed system at a particular temperature containing a solid or a liquid phase of a single chemical component, a gas phase will be formed at the equilibrium vapor pressure. Vapor pressures greater than 10^{-3} atmosphere can be measured directly. The most commonly used methods for direct measurements of vapor pressures use the Bourdon tube or Sickle gauge, the rise of a liquid manometer, the formation of bubbles, and so forth. One can also determine the boiling point, dew point, or vapor density, which can be related to the vapor pressure. Except for a few low-boiling metals, the direct method cannot be used very successfully for metallic systems, primarily due to the required high temperatures of measurement and reaction of the metallic vapors with the container.

The most important indirect methods of determining vapor pressures are:

(a) The mass spectrographic method

(b) The mass transport method from about 10^{-5} to greater than

10^{-3} atmosphere

(c) Langmuir's method from about 10^{-10} to 10^{-3} atmosphere

(d) The methods of Knudsen and torsion effusion from about 10^{-7} to 10^{-3} atmosphere

In the mass spectrographic method the molecules of the vapor phase are ionized to +1 ions by electron bombardment, and the vapor pressures are obtained from measurements of the number of these ions. It is difficult to obtain accurate vapor pressures by this method due to the uncertainty of the degree of ionization. The mass spectrograph is most helpful in determining the molecular weights of the gaseous molecules.

In the transport method a flow of inert gas is passed over the vaporizing component at a constant temperature and constant total pressure; the vapor is commonly condensed, collected, and weighed. From this can be calculated the mol fraction and partial pressure of the vapor in the inert gas. For sufficiently slow flow rates the pressure found should be near equilibrium, though the method is complicated by diffusion of the vapor through the gas. This method is reliable only when care is taken to test whether the rate of flow is slow enough to allow equilibrium and fast enough to avoid important contributions of thermal diffusion. Care must also be taken to avoid reactions with impurities in the gas, with the containers, etc.

Langmuir[1] first determined the vapor pressures of tungsten, molybdenum, and tantalum from measurements of the rate of weight

loss per unit area into a vacuum. From these data the equilibrium vapor pressures were calculated in the following way:

Suppose a sample at temperature T is surrounded by its vapor at the equilibrium pressure, P. Under these conditions the number of vapor molecules which strike the condensed phase and stick to it equals the number which evaporate from the surface in the same time. From kinetic theory it can be shown that the rate of striking the surface

$$\nu = P\bar{c}/4kT \quad \text{molecules/cm}^2\text{sec.} \tag{1}$$

where $\bar{c}$ = average velocity. But only a fraction, α, of these molecules stick. α is called the accommodation or sticking coefficient. Hence at equilibrium

$$\nu\alpha = \text{number sticking} = \text{number escaping} = \alpha P\bar{c}/4kT \tag{2}$$

The mass of a molecule is M/N where M is the molecular weight and N is Avogadro's number. From kinetic theory it may be shown that

$$\bar{c} = \sqrt{8NkT/\pi M} \tag{3}$$

Hence:

$$\nu\alpha\, M/N = \text{mass sticking} = \text{mass escaping} = m = \alpha MP\sqrt{8NkT}/4NkT\sqrt{\pi M}$$
$$= \alpha P\sqrt{M}/\sqrt{2\pi RT}$$

So that $$P = \frac{m}{\alpha}\sqrt{\frac{2\pi RT}{M}} \tag{4}$$

The equilibrium vapor pressure can thus be determined from the weight loss, m, per second from unit area if the molecular weight, M, of the vapor and the sticking coefficient, α, are known. Fortunately, for most metals α is nearly equal to one and the vapors are monatomic.

In the Knudsen[2] method vapor pressures are also determined from rates of weight loss of samples. Because of certain technical advantages it has to a large extent replaced the Langmuir method. In particular, the sticking coefficient, α, need not be known in the Knudsen method.

The sample is contained in a small, nearly closed container, the Knudsen cell, in which the equilibrium vapor pressure is developed. The vapor escapes from the cell through a tiny orifice of area a. If the orifice is small enough, the pressure of the vapor in the cell is not reduced appreciably. The mass of vapor, m, escaping per second will be

$$m = Pa\sqrt{M/2\pi RT}$$

$$P = (m/a)\sqrt{2\pi RT/M} = (m/44.331a)\sqrt{T/M} \qquad (5)$$

This applies for an infinitely thin knife-edged orifice in which the pressure is low enough so the mean free path of the escaping molecules is at least ten times the orifice diameter.

Real Knudsen cells deviate somewhat from the ideal behavior sketched above. All the factors are not fully understood. Clausing[3] derived a correction for the channeling effect due to thickness of the knife edges of the hole. Speiser and Johnston[4] considered the loss of pressure due to the hole as affected by the rate of evaporation from the surface area of the sample, and Motzfeld[5] made a more detailed analysis of the action of the Knudsen cell. In the present work the sample area was large compared with the hole size, since small solid particles were used, and only the Clausing correction needed to be applied. (See appendix)

II. TORSION EFFUSION METHOD

The torsion effusion method is the one which has been mainly used to determine the activities of manganese in iron-manganese alloys in the present investigation. It consists of measuring directly the recoil force exerted by the effusing vapor through small orifices into a surrounding vacuum. The apparatus consists of two main parts, (1) the vacuum system and furnace assembly (Fig. 1), and (2) the suspension system (Fig. 2). The suspension system is the part which distinguishes this apparatus from the Knudsen effusion method. It consists of a fine wire or ribbon, one end of which is attached rigidly to the top of the apparatus and the other to the freely suspended crucible assembly which is held in the hot zone of the furnace. During the run the effusing vapor from the eccentrically placed holes in the cell causes the suspension to rotate until the impulse momentum is balanced by the torque of the suspension wire. The torque can be measured from the angle of twist, which is proportional to the torque in the elastic range. The amount of torque produced can be correlated with the cell geometry to obtain the vapor pressure of the sample in the following manner:

$$P = \frac{2 D \phi'}{a_1 q_1 + a_2 q_2} \qquad (6)$$

where D = torsion constant of the suspension filament

ϕ = angle of rotation

a_1 and a_2 = area of the infinitely thin effusing orifice

q_1 and q_2 = distance of the orifices from the axis of rotation.

However, in practice we always have a finite thickness of the hole which will cause a channeling effect somewhat similar to that of the Knudsen effusion, so we have to consider a correction factor for torsion effusion. The correction factor derived by Clausing[3] takes into account only the probability of a molecule which has entered one end of the hole of finite length escaping into the vacuum system. This correction is sufficient in Knudsen effusion since the weight loss depends only on the number of molecules which escape. However, when we are considering the forces exerted due to the effusing vapor the situation is slightly different. Searcy and Freeman[6, 7] took into consideration the angular distribution of velocities of the effusing molecules since the torsional vapor pressure calculated from the force exerted by the effusing molecules depends not only on the number of escaping molecules but also on the angular distribution, and when this is taken into consideration in equation 6 we have the final torsion equation as

$$P = \frac{2 D \phi}{f_1 a_1 q_1 + f_2 a_2 q_2} \qquad (7)$$

where f_1 and f_2 are the force correction factors calculated by Searcy and Freeman.

The torsion method has several advantages over the other methods of determining vapor pressures of pure metals and alloys:

(a) Torsion effusion measurements are faster than those by the weight loss method.

(b) Vapor pressures can be determined without the knowledge of the molecular species in the vapor phase.

(c) The uncertainty associated with the heating and cooling time in the weight loss method is avoided.

The first advantage is of particular importance in alloy systems where depletion of the surface is a factor. Measurements by weight-loss (or collection) techniques can be made only after considerable material has been vaporized, hence, after considerable depletion. The torque measurement may be made very quickly after the specimen comes to temperature at a time when minimum depletion has occurred. More important, continuous measurements may be made so that depletion can be readily detected and, perhaps, allowed for.

Vapor pressures measured by any of these methods may be converted into thermodynamic quantities as described in the next section. If one component is much more volatile than the other (say P_B greater than $100P_A$) the total measured pressure may be considered equal to the partial pressure of that component, and the partial molar quantities for B may be determined from the measurements. By Gibbs-Duhem integration it is then possible to determine the quantities for the other component and, of course, the integral quantities for the system.

Where both components are volatile enough to contribute significantly to the vapor pressure, it is necessary to determine the composition of the vapor. This might be done, for example, by a chemical analysis of the condensate of the vapor. In this case, independent determinations have been made of the vapor pressures of both components. The Gibbs-Duhem condition then furnishes a valuable check on the accuracy of the determinations.

III. THERMODYNAMICS

In a binary alloy of composition $A_{1-x}B_x$ the activity at a particular composition and temperature equals

$$a_B = \frac{P_{B\ in\ alloy}}{P^{\circ}_{B(pure)}} \tag{8}$$

if the vapor behaves ideally.

The activity co-efficient $\gamma_B = \frac{a_B}{x}$ (9)

The relative partial molar Gibbs energy is given by

$$\Delta\bar{G}_B = R\ T\ \ell n\ a_B \tag{10}$$

and the excess Gibbs energy by

$$\Delta\bar{G}_B^{xs} = R\ T\ \ell n \gamma_B. \tag{11}$$

If the values of $\Delta\bar{G}_B^{xs}$ over the entire composition range of the alloy are known at a particular temperature, $\Delta\bar{G}_A^{xs}$ can be determined from the Gibbs-Duhem relation

$$d\Delta\bar{G}_A^{xs} = -\frac{x}{1-x} \cdot d\Delta\bar{G}_B^{xs} \tag{12}$$

From the temperature dependence of $\Delta\bar{G}_B^{xs}$ can be obtained the partial molal excess entropy $\Delta\bar{S}_B^{xs}$ of component B from the relationship

$$\frac{d\Delta\bar{G}_B^{xs}}{dT} = -\Delta\bar{S}_B^{xs} \tag{13}$$

Similarly $\Delta\bar{S}_A^{xs}$ can be obtained from the Gibbs-Duhem relationship. From both partials the integral thermodynamic properties can be obtained from the relationships

$$\Delta Y^{xs} = (1-x)\,\Delta\bar{Y}_A^{xs} + x\Delta Y_B^{xs} \tag{14}$$

$$\Delta Y = \Delta Y^{id} + \Delta Y^{xs} \tag{15}$$

and

$$\Delta H = \Delta G + T\Delta S \tag{16}$$

where Y = any thermodynamic property and Y^{id} its ideal solution value. In order to carry out the Gibbs-Duhem integration of the partial quantities it is easier to introduce two functions α_B and β_B,

$$\alpha_B = \frac{\Delta\bar{G}_B^{xs}}{x_A^2} \tag{17}$$

$$\beta_B = \frac{\Delta\bar{S}_B^{xs}}{x_A^2} \tag{18}$$

The Gibbs-Duhem relation in terms of α_B becomes

$$\alpha_A = -\frac{x_A}{x_B}\alpha_B + \frac{1}{x_B^2}\int_0^{x_B}\alpha_B\, dx_B \tag{19}$$

and

$$\Delta\overline{G}_A^{xs} = -x_A x_B \alpha_B + \int_0^{x_B}\alpha_B\, dx_B \tag{20}$$

Similar relations hold for β_B, β_A, and $\Delta\overline{S}_A^{xs}$.

IV. THE APPARATUS

The apparatus was designed so that it could be used for both the torsion and Knudsen methods. The furnace chamber (Fig. 1) consists of a stainless steel cylinder (A) 14 inches in diameter and 15 inches long. Stainless steel was used because of its smooth surface which cuts down the amount of absorbed gas and consequently the pumping time. The furnace chamber is water-cooled by copper tubes (B) soldered outside the shell. In the center of the top plate there is a one-half inch hole, (C), surrounded by a concentric "O" ring groove which is used as the upper port for the passage of the suspension system (D), and also as an optical window for the optical pyrometer in the case of Knudsen measurements. A six-inch-diameter right-angle-bend pipe (E) is welded to the side of the chamber, which is connected to a CVC MCF 700 type oil diffusion pump and a mechanical pump through a nitrogen trap.

The bottom plate of the chamber has three holes. One is for the inlet of the tungsten-rhenium thermocouple (F_1) which is introduced through a glass-metal 'KOVAR' type seal. The thermocouple was welded with a plasma jet. The two other holes (F_2 and F_3), which are one inch in diameter, are used for leading in two pairs (G_1 and G_2) of 1/4 inch copper tubes through rubber seals. These two pairs of copper tubes are water-cooled and are used as electrical conductors to bring the current into the chamber. Each pair of copper tubes (for inflow and outflow of water) is connected to a hollow circular

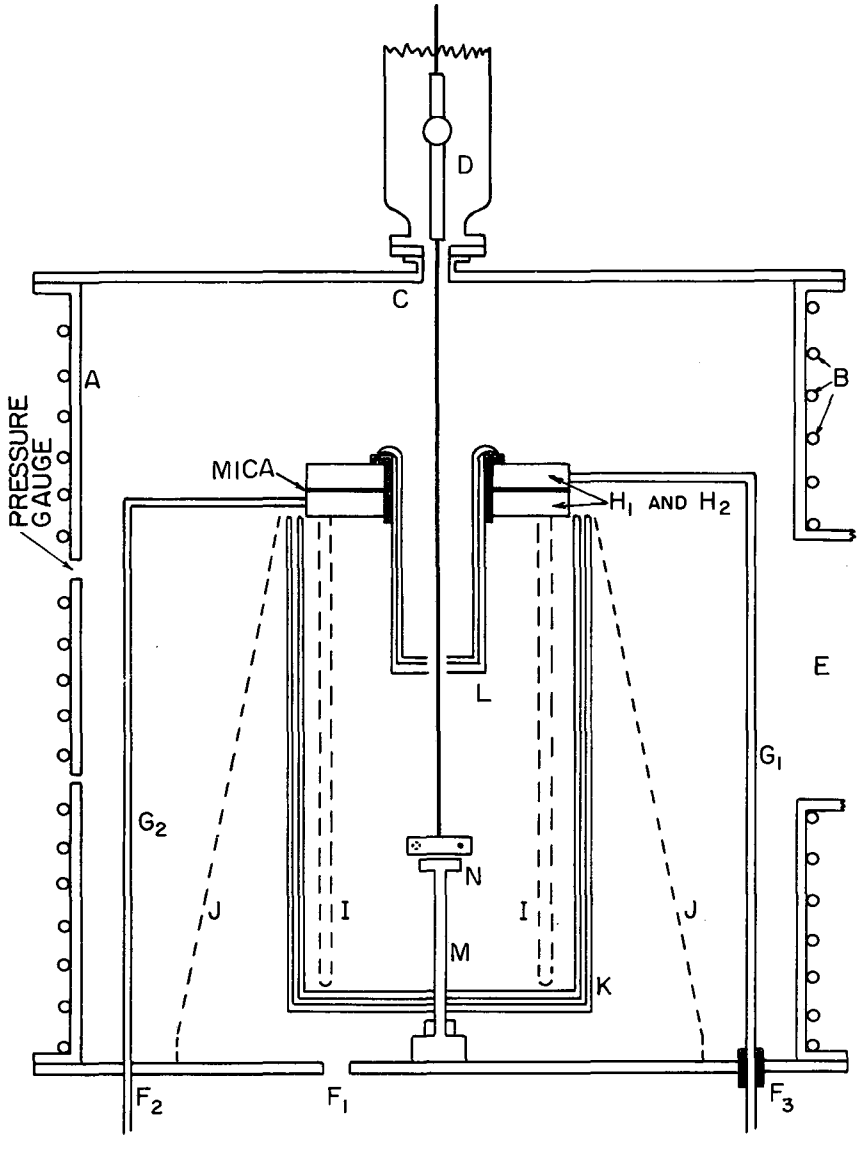

FIG. I FURNACE ASSEMBLY.

MUB-4063

disc (H_1 and H_2) 5 inches in diameter and 9/16 inch thick with a 2 inch diameter hole at the center. The copper discs are placed on top of each other with a mica insulation between. Ten sixty-mil diameter tungsten hair pins (I) about 11 inches long (which are used as heating elements) carry the current between the two copper discs. The heating elements with the two copper discs are supported on a tripod stand (J) inside the vacuum chamber. A set of four radiation shields (K) (the inner one of tantalum and the remainder of molybdenum) is used to surround the heating elements. A set of three radiation shields (L) is placed through the top opening of the water cooled circular copper plates. These top radiation shields have a one-quarter inch hole at the center for the passage of the torsion cell. The bottom radiation shields also have a 3/16 inch hole for the passage of an alumina tube (M) which is used as a stand for the dummy cell(N) and also the Knudsen cell. The tungsten-rhenium thermocouple is brought into the hot zone through the tube. The 220 volt input is controlled by a 7 KVA powerstat, then stepped down by twelve 0.575 KVA transformers in parallel, each with a maximum output voltage of ten volts. Temperature control is achieved through a Leeds and Northrup controller actuated by a signal of the thermocouple. A safety switch which is operated by the input water pressure to the furnace is placed in series with the input power. With this arrangement a maximum sample temperature of about 1700° C may be attained.

With a larger available power source it would be possible to use a furnace of this type for temperatures up to about 2100° C.

The suspension system shown in Fig. 2 is enclosed in a 2 1/2 inch diameter by a 28 inch tall Pyrex tube (O). A copper-to-glass seal (P) joins the tube to a brass flange which is sealed by an "O" ring to the upper part of the furnace. The upper part of the glass tube has a similar flange with a 1/4-inch Sealastic fitting at the center. The torsion filament is suspended from a 14-inch long and 1/4 inch diameter brass rod (Q), the lower end of which is in the vacuum system and has a chuck for holding the torsion filament (Q_1). The Sealastic fitting (R) allows the rotation of the brass rod without any loss of vacuum. The upper end of the brass rod extends out and is connected to a reduction gear mechanism (S). The 360 to 1 reduction mechanism is coupled with a counter and permits a rotation of 0.01 degree interval. The rotating device is operated manually at a convenient height by means of two coupling gears (U). A torsion filament (T) of either 2 mil diameter circular tungsten wire or a ribbon of 1 by 4 mil cross section was used for the experiment. Since recrystallized alumina crucibles were used and the cell assembly in operation weighed more than 120 grams, it was not possible to use thinner wires such as those normally used for graphite cells. Since the sensitivity decreases as the fourth power of the suspension wire diameter, sensitivity has to be sacrificed in order to support the

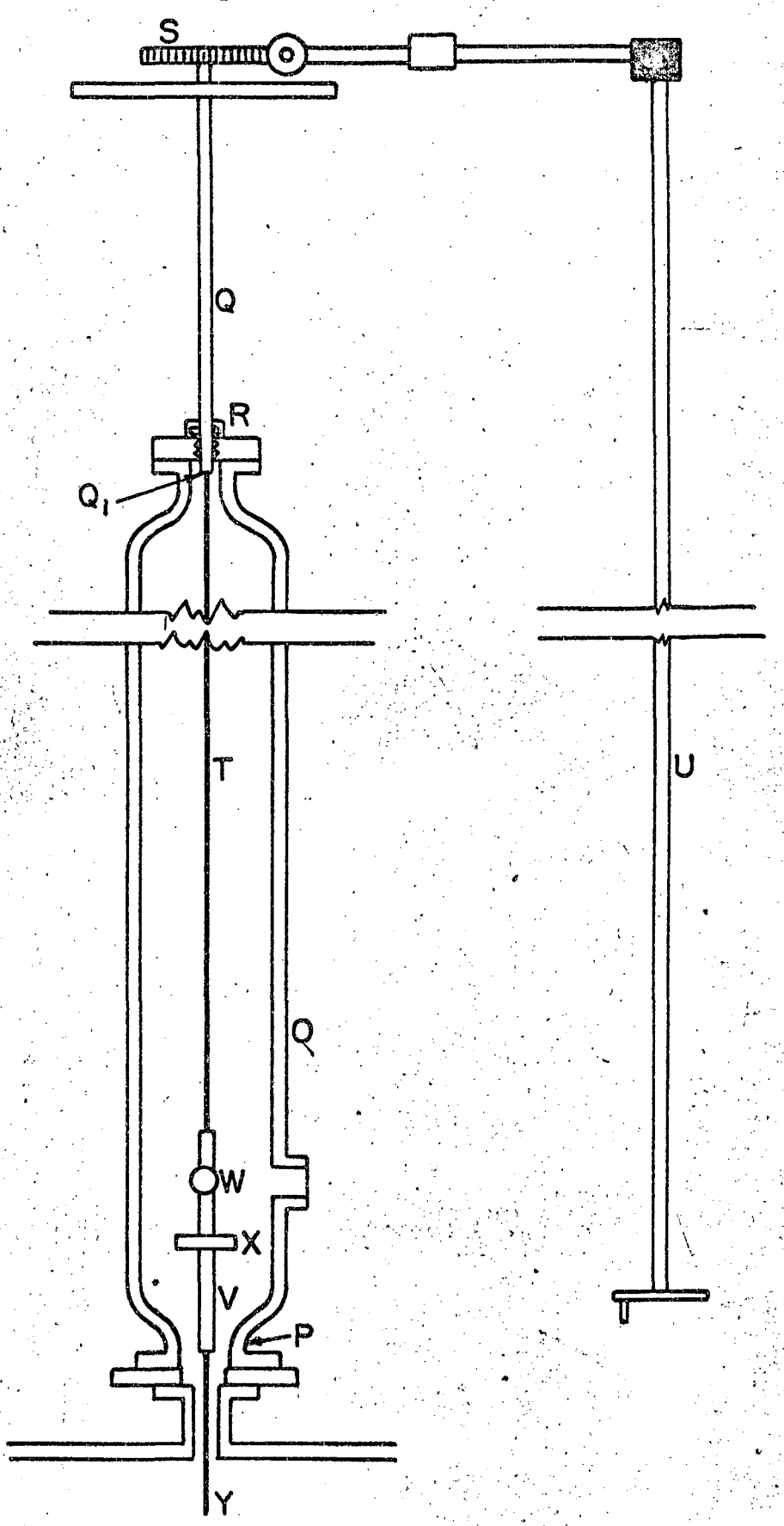

FIG. 2 SUSPENSION SYSTEM.

load without surpassing the elastic limit of the suspension wire. The ribbon torsion filament of rectangular cross section (obtained from H. Cross Company) was used to increase the sensitivity.[8] Although ribbon has been used extensively in galvanometers, it has never been used in torsion experiments. It seems from the present investigation that up to a deflection of about 90° the ribbon performs ideally. Residual distortion after a run was less frequently observed with ribbons than with circular wire, which may be due to better uniformity of the dimensions of the ribbon throughout the entire length of the ribbon torsion filament. A tungsten ribbon instead of a circular wire is highly recommended for torsion work. Each of the torsion filaments was about 23 inches long. No great increase of sensitivity would be attained by increasing this length. Because of its good quality with regard to tensile strength and modulus of rigidity, tungsten was chosen as the torsion filament material.

A 1/4 inch diameter aluminum rod (V) 6 inches long with chucks at both ends is used to suspend the torsion cell assembly from the torsion filament. A front-surfaced galvanometer mirror (W) is glued 2 inches from the top of this rod and serves as a deflection measuring device. Located two inches below the mirror is an aluminum damping disc (X). It is 1-1/4 inches in diameter, 1/2 inch thick, and has a 1/4 inch hole through the center which permits a tight friction fit between the rod and the damper. The lower end of this

aluminum rod is attached to a 60 mil tantalum rod (Y) of about 13 inches length. This rod extends into the furnace chamber where at the lower end the torsion cell block (Fig. 3) is attached.

Care was taken to avoid any ferromagnetic material in the suspension system, since it could be affected by either the electromagnetic field of the furnace or the damping magnet. The torsion constants of the 2 mil wire and the 4 x 1 mil ribbon were 1.6 and 1.02 dyne cm^{-1} rad^{-1} respectively. The torsion constants were measured by timing the period of oscillation with added weights of known moments of inertia. This information enables the torsion constant of the wire to be calculated:

$$D = \frac{4\pi^2 (I_1 - I_2)}{t_1^2 - t_2^2} \tag{21}$$

where

I_1, I_2 = Moments of inertia of the weights

t_1, t_2 = Periods of oscillation with the weights.

Due to the initial relaxation of the torsion filament, it was necessary to keep the filament under the load for a few days before using in order to ensure that the torsion constant did not vary during the runs.

Recrystallized alumina was used for the torsion cell because of its impervious nature and its resistance to reaction with the manganese vapor. Since manganese vapor is very reactive at high temperatures, a molybdenum or a tantalum cell might act as a sink

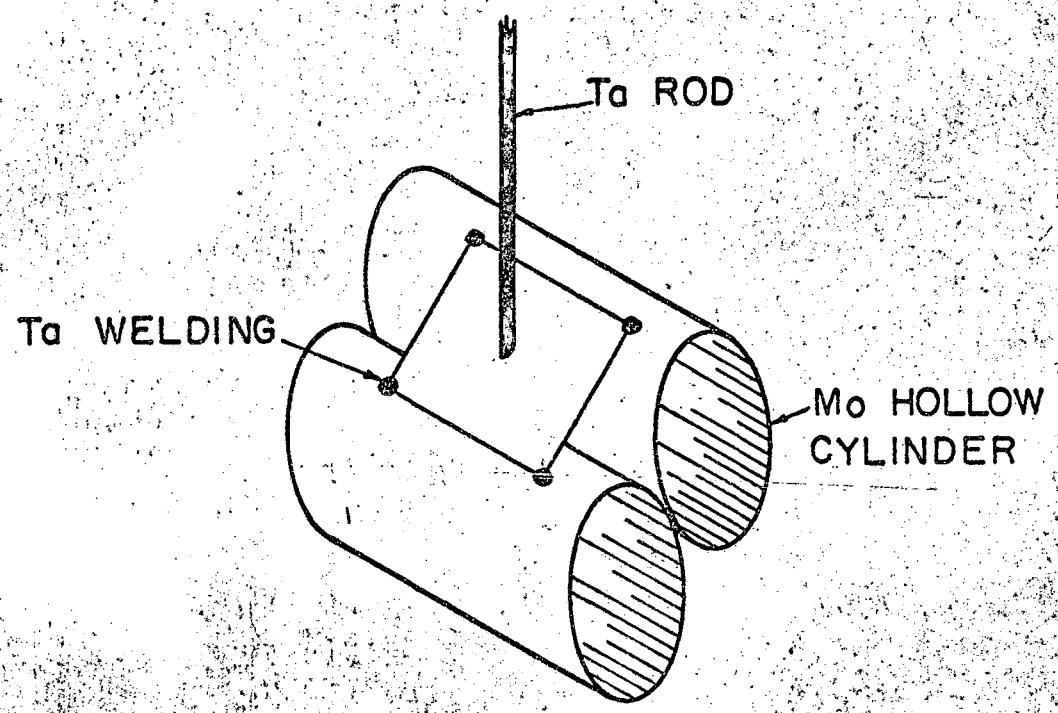

TORSION CELL HOLDER

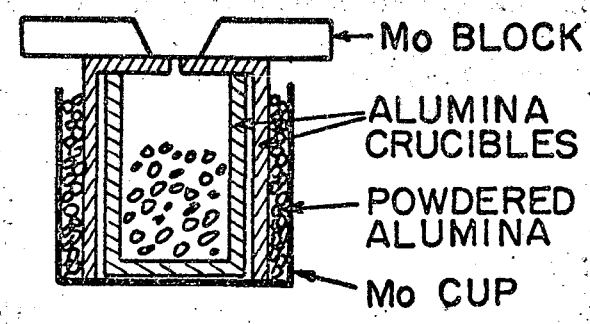

KNUDSEN CELL

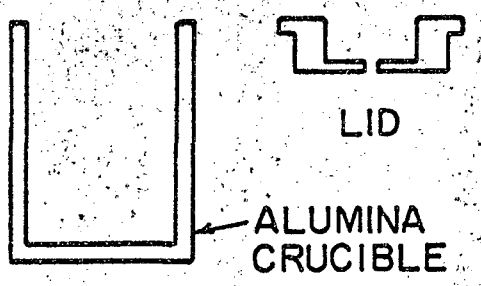

TORSION CELL

FIG. 3

for the vapor and make it difficult to attain the equilibrium pressure inside the cell. Two very thin molybdenum cylinders were welded together and to a 60 mil diameter tantalum rod to form the crucible holders (Fig. 3). This was done in order to keep the geometry of the cell fairly rigid. The crucible lids (Fig. 3) were machined with a slight taper with diamond tools so that they fit very snugly on the top of the crucible. The crucibles were placed in the hollow molybdenum cylinders with the holes facing in opposite directions and were secured in place by wedging them with thin molybdenum sheets.

One of the problems was the difficulty in determining the exact correction factor for the orifice drilled in the alumina crucible lid; it is difficult to machine a very small uniformly cylindrical hole. When supersonic drills were used to make the holes, they inevitably became tapered and eccentric. This made it impossible to calculate exactly the area and the channeling effect correction factor. However, the vapor pressures of pure manganese calculated from the torsion constant data and the approximate hole area agreed with the literature values within 10 to 20 percent depending on the hole size, indicating that the setup in general was performing satisfactorily.

In this investigation the deflection was measured by the null point method. After the mirror was deflected by the vapor pressure torque, it was returned to its original position by manually operating the gear mechanism at the top of the suspension system. Thus the

angle required to return the mirror to its original position is equal to its angle of deflection. The angle could be read to the nearest 0.01 degree. The precision of the measurements was found to be ±0.025 degree; the error was due to temperature fluctuation and vibration of the cell. A light and a scale were placed at a distance of about five feet from the mirror. Since the deflection was measured by a null point method, it was not necessary to calibrate the traverse length of the reflected beam on the scale per degree of rotation; it was about 10 cm per degree.

V. MATERIALS

Electrolytic iron and manganese of 99.95 percent purity were used for the preparation of the alloys. Twelve alloys of about 800 grams each containing 9 to 80 percent manganese were melted in an induction furnace in alumina crucibles under helium atmosphere. The alloys were poured into a water-cooled copper mold. Since the liquidus and solidus temperature differences in the iron-manganese system (Fig. 4) are very small, the very rapid quenching should lead to negligible segregation in the alloy. Electron probe analysis was carried out on some of the quenched samples and no inhomogenity was observed. The 70 and 80 percent manganese alloys were very brittle and the ingots shattered during quenching. Most of the alloys were sawed, and the sawed particles (0.001 to 0.5 mm) were used for the experiment; the 70 and 80 percent alloys were crushed before using. Fine particles were used in order to increase the ratio of the surface area of the alloys to that of the orifice. About 1/8 inch of the alloy was machined off from the surface of the ingot and discarded. The top, middle and bottom sections of the ingots were then chemically analyzed. The manganese analysis was carried out in this laboratory by potentiometer titration as described by Lingane and Karplus.[9] The iron analysis was done by dichromate titration. The precision of the ultimate determination of the composition was about ±0.3 percent. Ten of the alloys were also analyzed by the Chemistry Division of the University of California, Lawrence Radiation Laboratory, and their

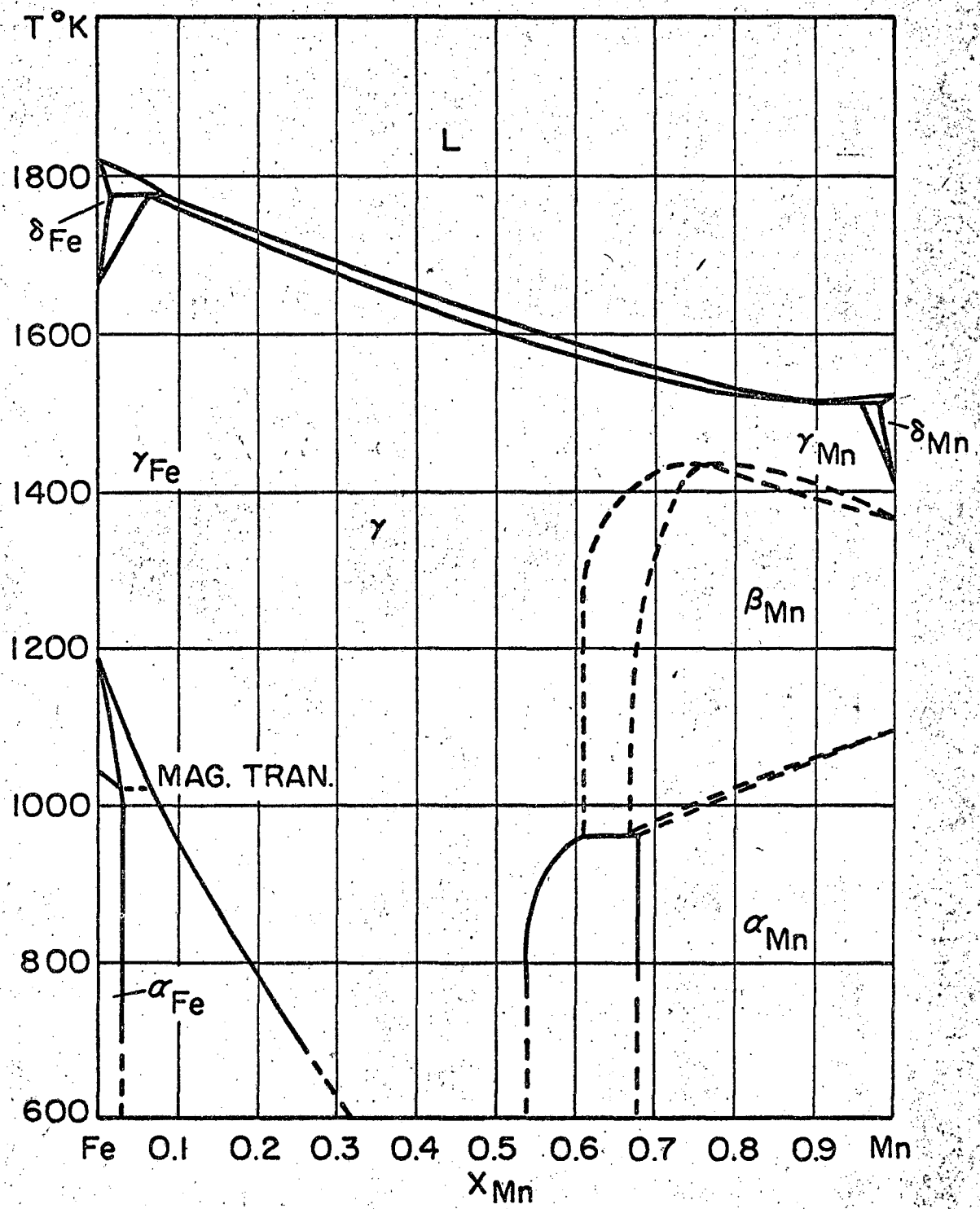

FIG. 4 IRON-MANGANESE SYSTEM.[22]

analyses checked within 0.5 percent with the analyses made in this laboratory. The average values of the analyses are given in Table I:

Table I

Manganese Content of Alloys

Alloy	x_{Mn}	Alloy	x_{Mn}
1	0.090 ± .001	7	0.452 ± .002
2	0.197 ± .002	8	0.499 ± .001
3	0.253 ± .002	9	0.548 ± .003
4	0.318 ± .001	10	0.597 ± .002
5	0.349 ± .002	11	0.700 ± .001
6	0.402 ± .001	12	0.802 ± .002

No weight loss correction was made for the torsion results, since the weight losses were very small (about 10^{-3} gm average) from the 10 gram of samples used for each run. Thus, the correction was less than the uncertainty of the manganese analyses. However, for the Knudsen results the weight losses were in the order of 0.09 grams and were taken into consideration; the average composition between the initial and the final fun after evaporation was taken to be the composition of the sample.

VI. EXPERIMENTAL PROCEDURE

The Knudsen effusion technique was first used to determine the vapor pressures of both pure manganese and the alloys. Two coaxial crucibles of recrystallized alumina were used as the crucible assembly; the crucibles were placed in a molybdenum cup, and the space between the crucibles and the cup was packed with alumina powder (Fig. 3). This was done because the facility for making snug fitting lids was not available at that time. To avoid the problem of geometry of the hole, the same crucible lids were used for both the pure metals and the alloys. The crucible was placed on a molybdenum block on an alumina stand, and the thermocouple was placed within 1/8 inch of the sample. The tungsten-rhenium thermocouple used was found to be quite suitable. Although in the temperature range of the measurement, Pt-Pt+10% Rh would have been satisfactory, the W-Re couple has a higher temperature coefficient and is more convenient. It was found to remain stable well above 1650° C, hence it is to be recommended for measurements of temperatures above the Pt-Pt+10% Rh limit. The thermocouple was calibrated by both an optical pyrometer and a standard Pt-Pt+10% Rh thermocouple. The uncertainty of the temperature is probably 1° to 3° C; however, since the vapor pressure measurements are relative, the absolute uncertainty in temperature will have little effect on the final results, as the same temperature calibration curve was used for both pure manganese and its alloys.

Crucibles with approximate hole areas of 0.0022, 0.0077 and 0.010 cm^2 were used for the measurements. However, the holes in the alumina, which were made by supersonic drills, were irregular so that the effective areas and the proper Clausing factors could hardly be determined accurately by measurement. Each hole was therefore calibrated by measuring the vapor pressure of pure manganese. For each crucible a correction factor was calculated. The Clausing factor times hole area was multiplied by the correction factor whose value was chosen to make the vapor pressure determined experimentally agree with that given in the literature.[10] The average correction factor for all the determinations from a given hole was then used to give an "experimental" value for P_{Mn}, and ΔH^{v}_{298} was calculated and shown to have no temperature dependence and to be consistent to ±150 cal/g-atom. The data are given in Table VI in the Appendix. The vapor pressures of alloys were then measured. In order to decrease the uncertainties introduced by weighing, it was necessary to have a weight loss in the order of 0.1 gram; the time required for a run was now so long that the corrections for the heating and cooling times became relatively insignificant. When there is a danger of surface depletion the weight loss should be kept to a minimum in order to obtain an equilibrium value. The results obtained by the Knudsen method are given in Table VI in the Appendix.

To test for depletion (which had also been found by McCabe et al.[11]), a torsion effusion cell was designed. In order to test the close fit of the lids a pure manganese sample was heated without any holes in the lids, and no deflection was noticed up to about 1500° K (where the expected pressure was 10^{-3} atm), which indicates that the seal was quite good. The torsion constants of the filaments were determined by the method described previously. The difference between the oscillation period in air and in vacuum was not significant when proper precautions were taken during the measurements.

Three hole sizes of approximate areas 0.0015, 0.0028 and 0.010 cm^2 were used. The theoretical calibration factors and the ones determined from the vapor pressure of manganese found in the literature[10] are given in Table II.

Table II

Calibration of Torsion Cell Assembly

Hole Area cm^2	Torsion Filament	Factor per degree of deflection	
		Calculated	Experimental
0.0015	Circular wire 2 mil diam.	34.7×10^{-6} atm	42.20×10^{-6} atm
	0.001" x 0.004" Ribbon	17.84×10^{-6} atm	21.70×10^{-6} atm
0.0028	Circular wire 2 mil diam.	20.58×10^{-6} atm	18.64×10^{-6} atm
	0.001" x 0.004" Ribbon	13.51×10^{-6} atm	12.24×10^{-6} atm
0.010	Circular wire 2 mil diam.	5.06×10^{-6} atm	5.64×10^{-6} atm

The calibration factor was not needed to determine activities, since the same crucible lids were used for both the alloys and pure manganese. Thus at a particular temperature, the activity is simply the ratio of the angles of deflection of the alloy and the pure component. However, the factor was determined in order to facilitate the evaluation of the data. The vapor pressures at all temperatures were then recalculated using the selected average factor. The heat of vaporization at 298° K obtained from the recalculated vapor pressures by the third law method agrees within ± 80 cal/g-atom with the literature value,[10] Tables IIIa to IIIf. This indicates that probably the absolute temperature measurement was quite good, since no temperature dependent error was noticed. The manganese runs were checked frequently, and the conversion factor remained constant provided the filament was kept loaded with the weights for a few days.

The tungsten-rhenium thermocouple was calibrated against a standard Pt-Pt+10% Rh thermocouple. The standard thermocouple was embedded in a 20 gram molybdenum block inside the torsion cell, and about 12 inches of the couple was wound around the cell to prevent heat loss through the leads. The W-Re couple was placed in the dummy cell which was kept at a constant distance of about 1/8 inch below the torsion cell during both the calibration and the experiments in order to avoid any uncertainty due to possible temperature gradients in the furnace. The temperature of the furnace was controlled within ±0.5°C.

After the alloys and the crucibles were washed with acetone, they were put in the crucible holder and the chamber was evacuated to a vacuum of 10^{-6} mm Hg. It was necessary before each run to wash the crucible and the lid with dilute nitric acid to dissolve manganese deposited on the cell wall. Several empty crucibles were put into the furnace and heated; no torque was noticed; therefore no volatile substance was in the cells. After several runs the crucibles seemed to become slightly tarnished. The tarnish disappeared when the empty crucibles were heated above 1500° C.

After loading the crucibles and evacuating the system, they were heated slowly to 200° C to remove any volatile impurities which might be present and to degas the sample. The crucibles were further heated to about 500 to 600° C and kept at that temperature for times up to 8 hours. Usually no deflection was observed at either stage.

During operation of the torsion effusion cell the depletion of the surface concentration of manganese discussed in the Introduction was directly observable. As the sample came to temperature, a torque in the suspension was developed; this decreased with time. The decrease was much too great to be accounted for by bulk depletion of manganese; measurable depletion occurred in samples with low manganese concentrations after the evaporation of only 10^{-6} grams of manganese.

The depletion was more pronounced the lower the manganese concentration and the higher the temperature of the run. For alloys

containing 40 atomic percent manganese and lower, torque readings were taken soon after attainment of temperature. In several cases at the higher temperatures it was necessary to provide a fresh sample for each run. For higher manganese contents it was possible to make readings at all temperatures without replacing the sample. The depletion effect is greater, as expected, with the larger hole diameters. As shown by the results (Figs. 5 - 10 and Tables IVa to IVℓ) consistent temperature dependences were found except at the highest temperatures and lower concentrations of manganese. It may be concluded, therefore, that with these exceptions, depletion has been practically eliminated as a factor in these measurements.

As with the Knudsen measurements, the torsion cells were calibrated by measuring vapor pressures of pure manganese (see page 29) Results of the calibration runs are shown in Tables IIIa to IIIf.

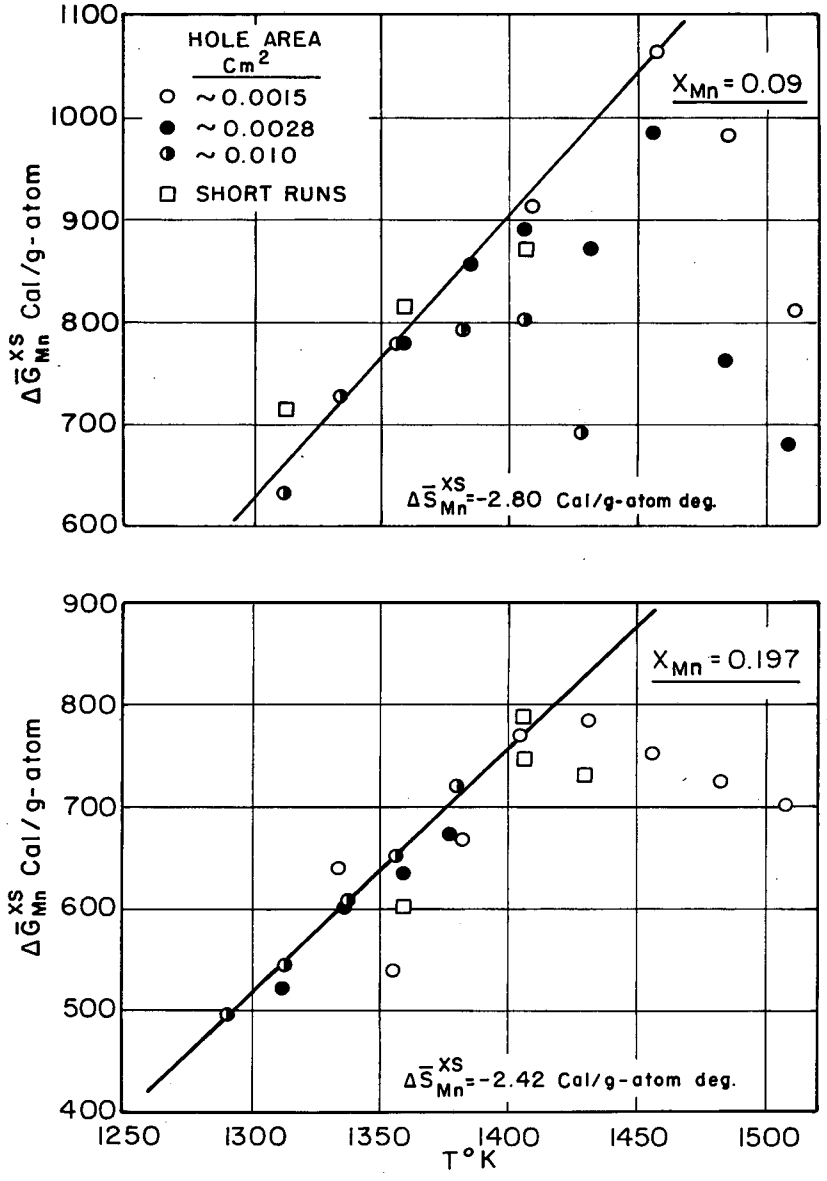

FIG. 5 EXPERIMENTAL VALUES OF $\Delta\bar{G}^{XS}_{Mn}$ FOR SOLID IRON-MANGANESE ALLOYS WITH RESPECT TO γ_{Mn}.

MUB-4064

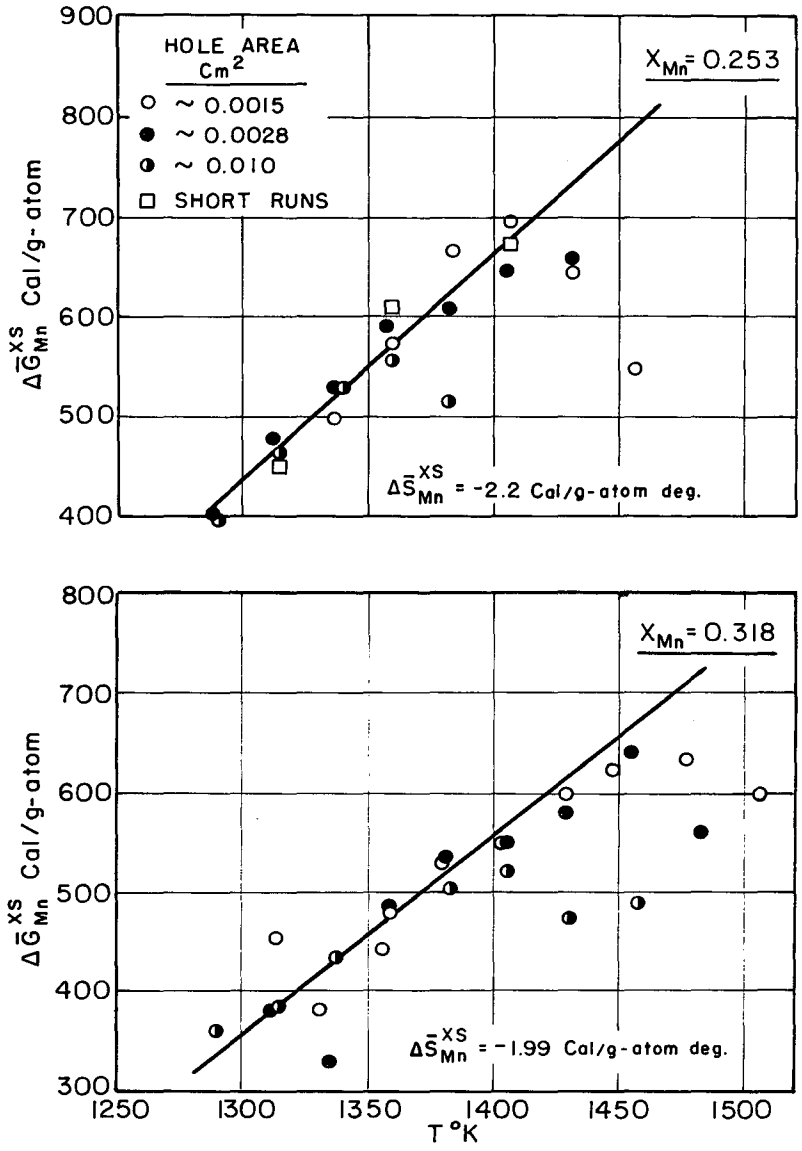

FIG. 6 EXPERIMENTAL VALUES OF $\Delta\bar{G}^{XS}_{Mn}$ FOR SOLID IRON-MANGANESE ALLOYS WITH RESPECT TO γ_{Mn}.

MUB-4065

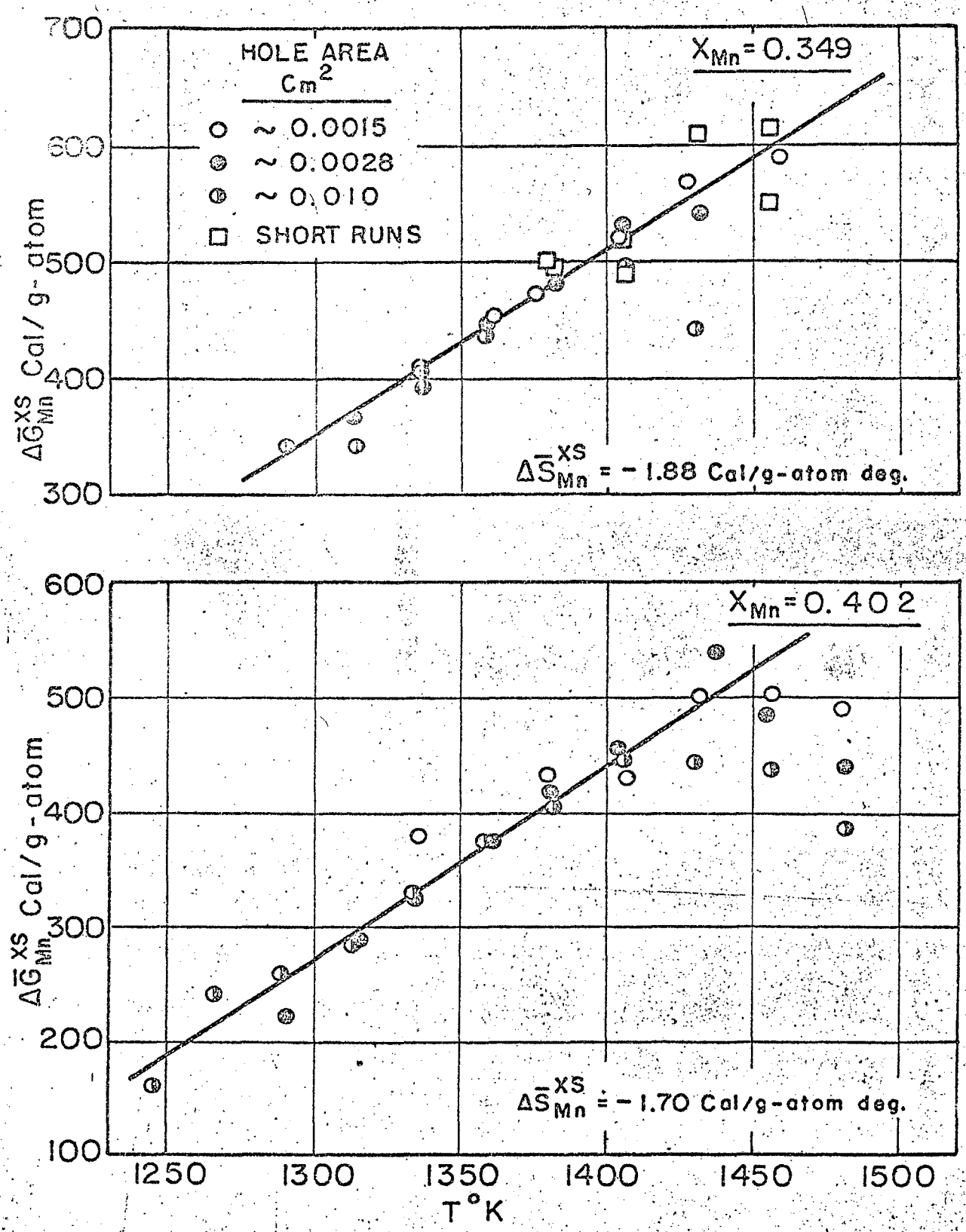

FIG. 7 EXPERIMENTAL VALUES OF $\Delta\bar{G}^{XS}_{Mn}$ FOR SOLID IRON-MANGANESE ALLOYS WITH RESPECT TO γ_{Mn}.

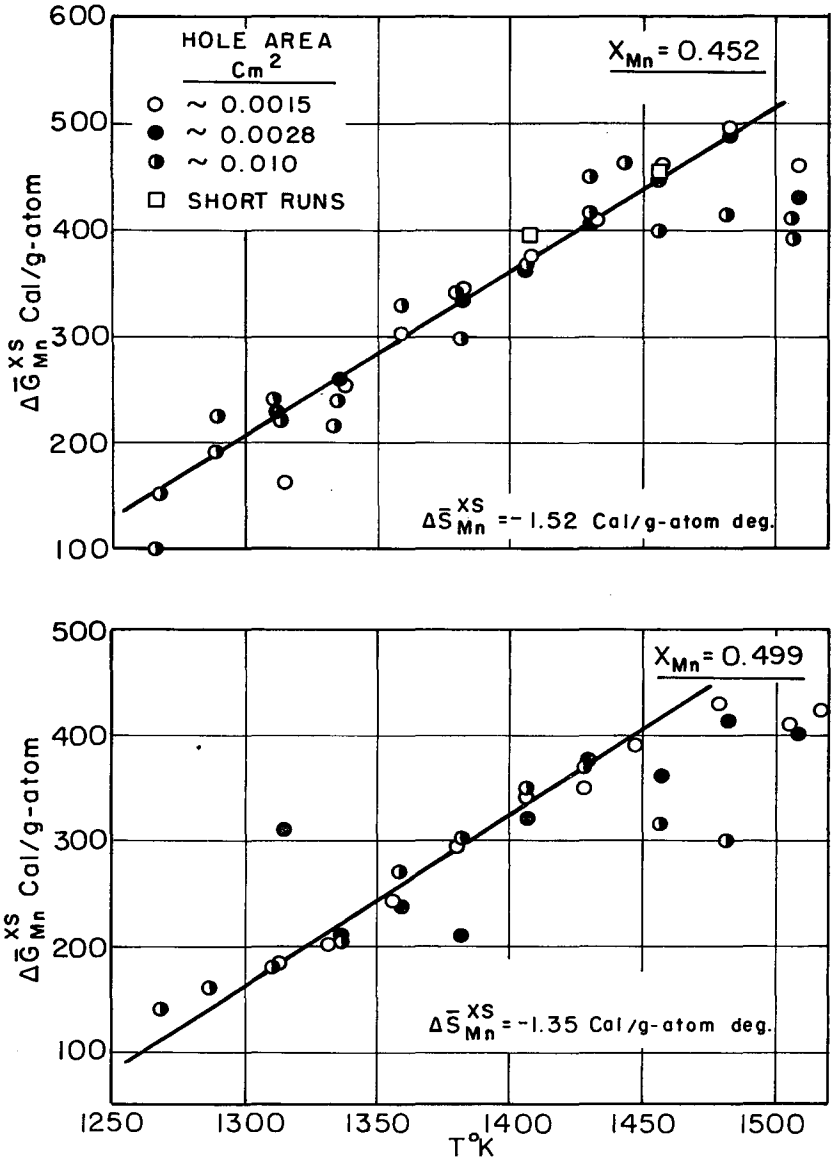

FIG. 8 EXPERIMENTAL VALUES OF $\Delta\bar{G}^{XS}_{Mn}$ FOR SOLID IRON-MANGANESE ALLOYS WITH RESPECT TO γ_{Mn}.

MUB-4066

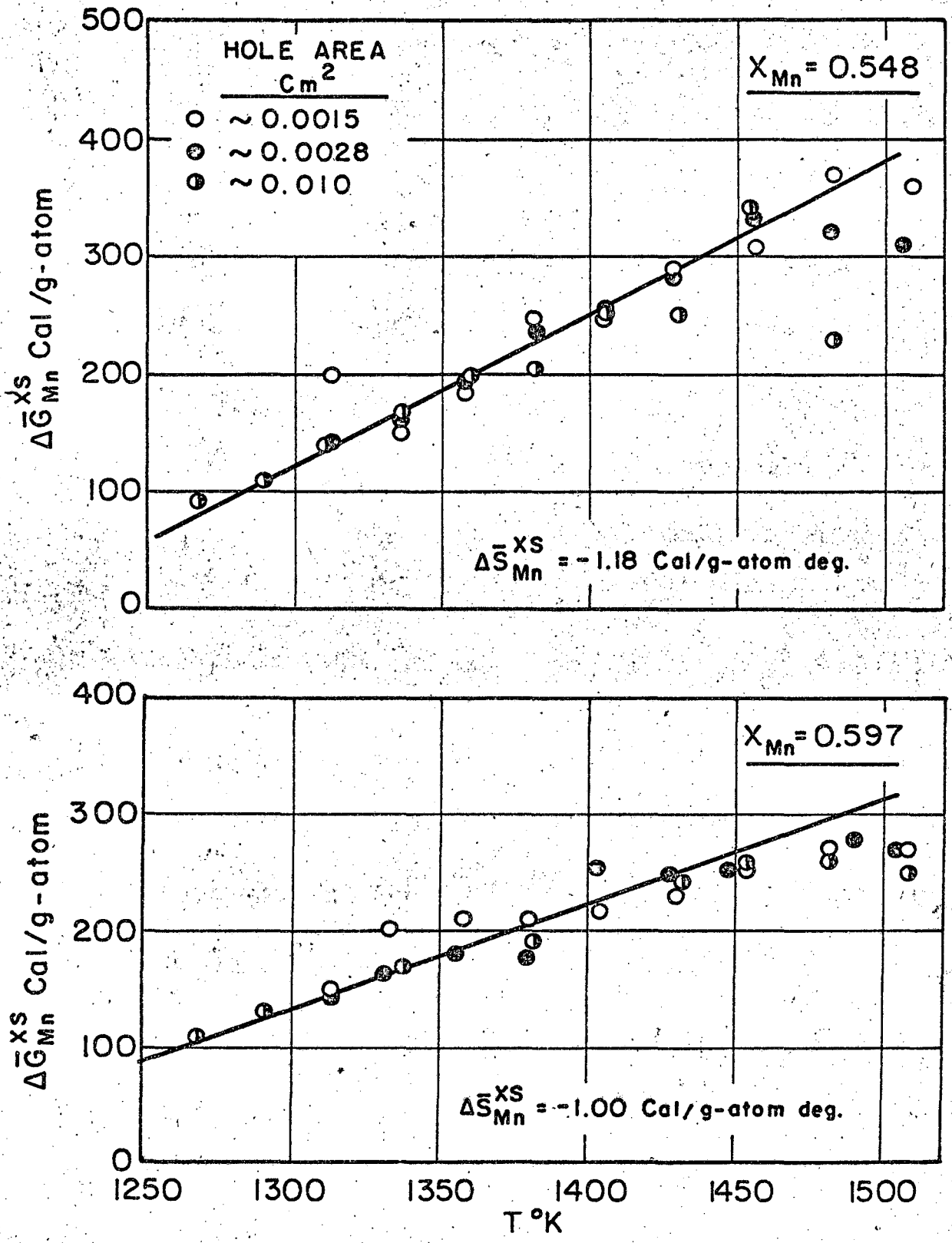

FIG. 9 EXPERIMENTAL VALUES OF $\Delta\bar{G}^{XS}_{Mn}$ FOR SOLID IRON-MANGANESE ALLOYS WITH RESPECT TO γ_{Mn}.

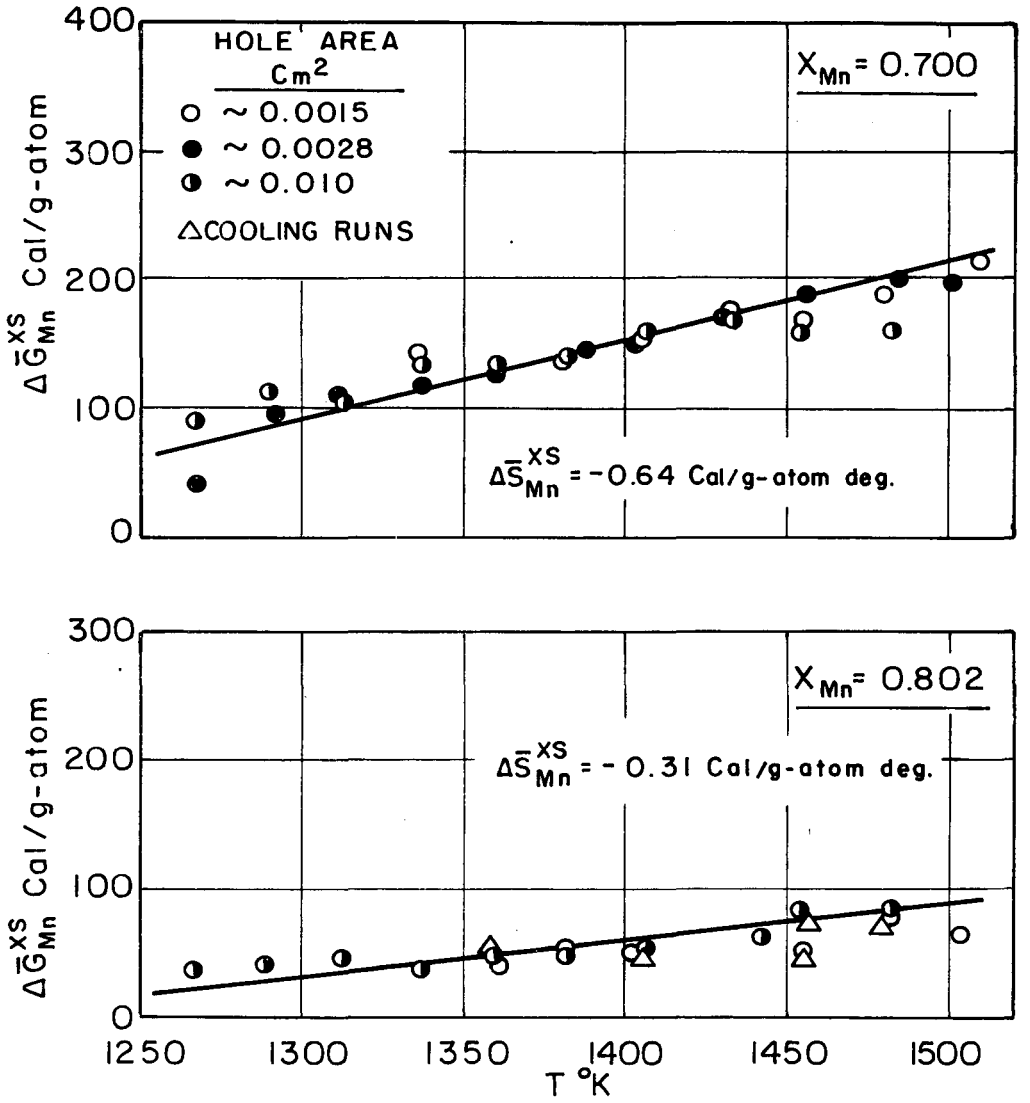

FIG. 10 EXPERIMENTAL VALUES OF $\Delta\bar{G}^{XS}_{Mn}$ FOR SOLID IRON-MANGANESE ALLOYS WITH RESPECT TO γ_{Mn}.

MUB-4067

VII. EXPERIMENTAL RESULTS

Experimental data are given in Tables IIIa to IIIf and IVa to IVℓ and VI (see appendix). Derived values of $\Delta\bar{G}^{xs}_{Mn}$ are plotted versus temperature in Figs. 5 - 10. Examination of these figures makes it quite clear that the higher values of $\Delta\bar{G}^{xs}_{Mn}$, are the most reliable. Higher values of $\Delta\bar{G}^{xs}_{Mn}$ correspond to higher vapor pressures. Large deviations are always in the direction of lower vapor pressures and can be explained as the effect of depletion. The effect of depletion increases with temperature, with lower manganese concentration, and with larger hole size, as would be expected.

Derived thermodynamic quantities as a function of concentration at 1450° K are shown in Figs. 11 - 15. Knudsen values of $\Delta\bar{G}^{xs}_{Mn}$ plotted in Fig. 12 were calculated from lower temperature measurements using the values of $\Delta\bar{S}^{xs}_{Mn}$ obtained from the torsion cell. The selected integral and partial molar quantities at 1450° K over the entire composition range are given in Tables V and Va and Figs. 14 - 15. Results of electron probe analyses are discussed in the next section.

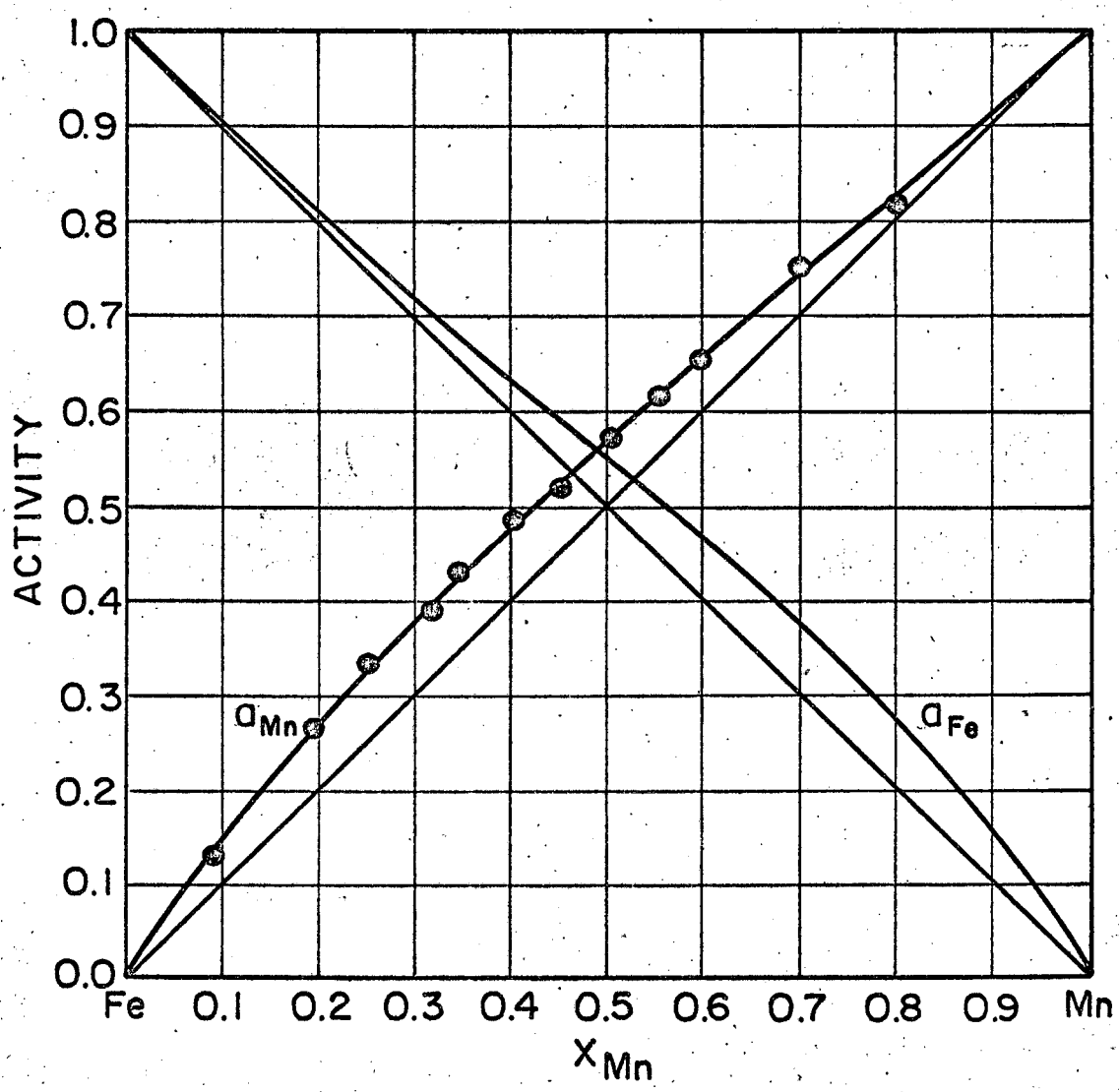

FIG. 11 a_{Mn} AND a_{Fe} FOR SOLID IRON-MANGANESE ALLOYS WITH RESPECT TO γ_{Mn} AND γ_{Fe} AT 1450 °K.

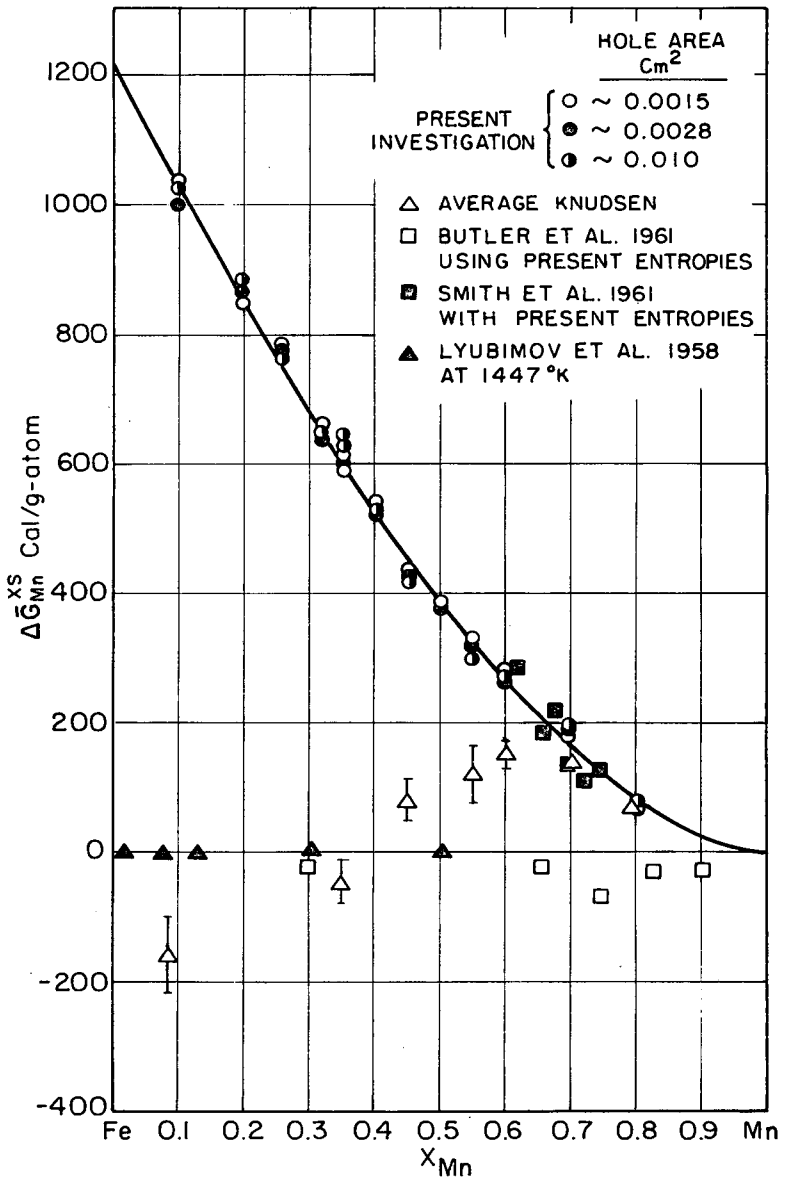

FIG. 12 $\Delta\bar{G}^{xs}_{Mn}$ FOR SOLID IRON-MANGANESE ALLOYS WITH RESPECT TO γ_{Mn} AT 1450 °K.

MUB-4068

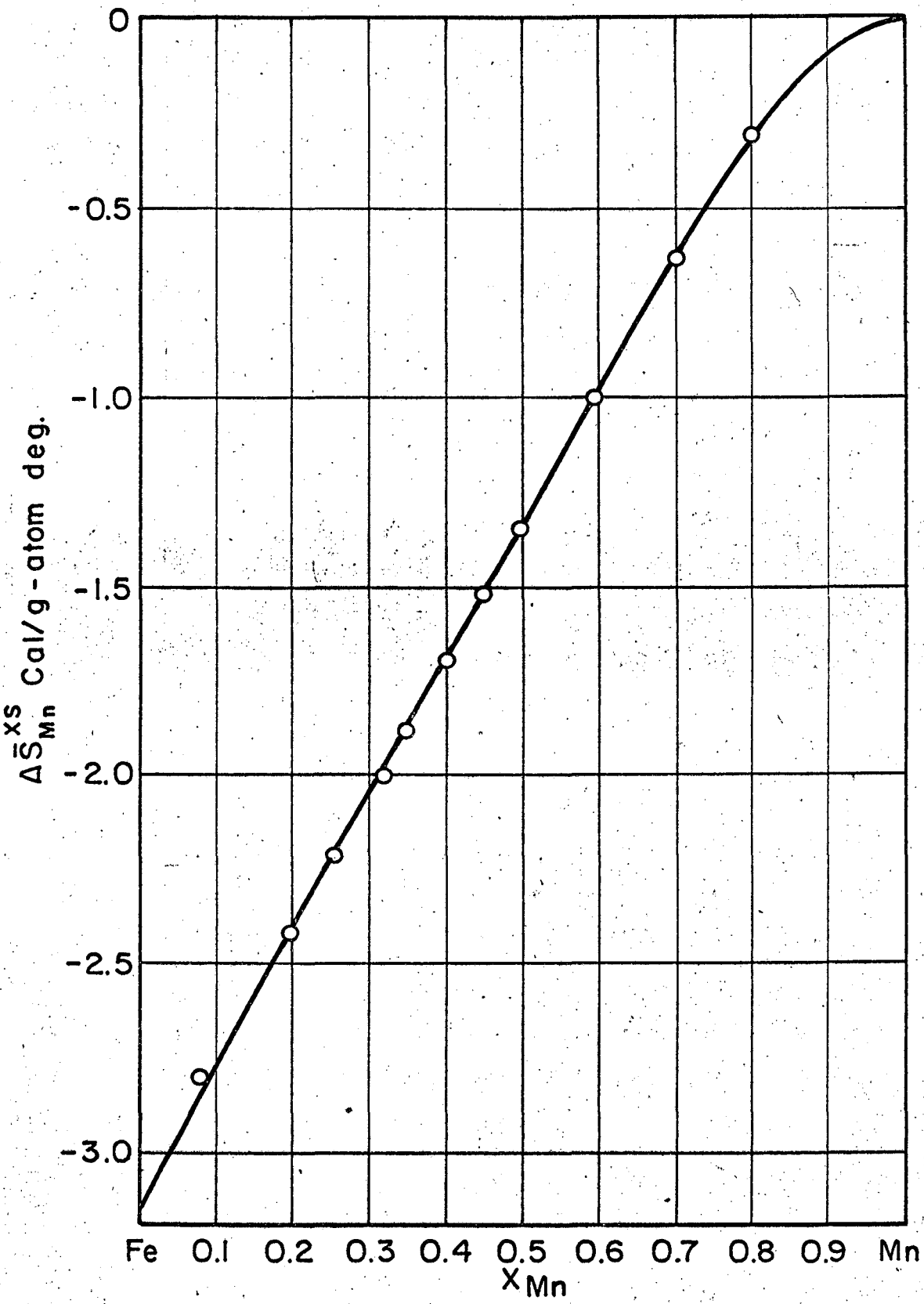

FIG. 13 SELECTED $\Delta\bar{S}^{xs}_{Mn}$ FOR SOLID IRON-MANGANESE ALLOYS.

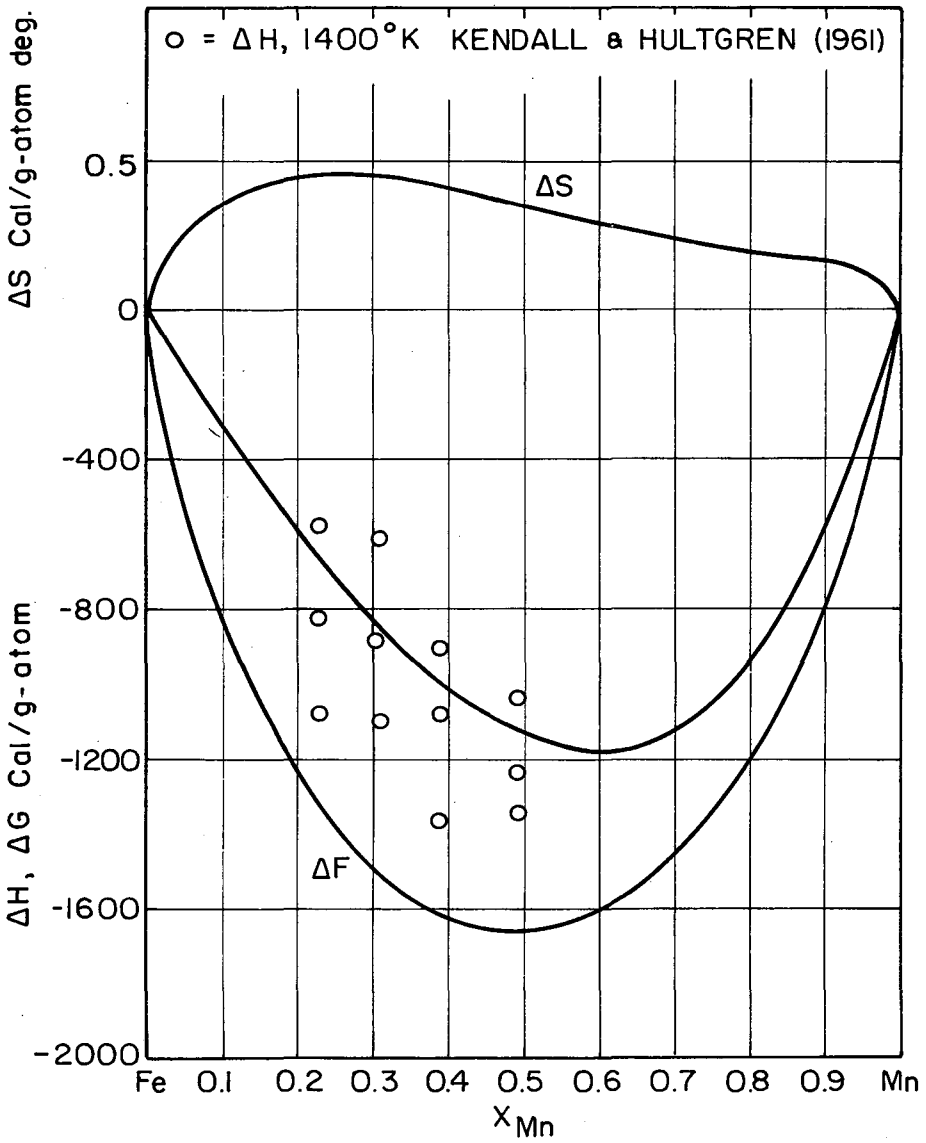

FIG. 14 INTEGRAL QUANTITIES FOR SOLID IRON-MANGANESE ALLOYS AT 1450°K.

MUB-4069

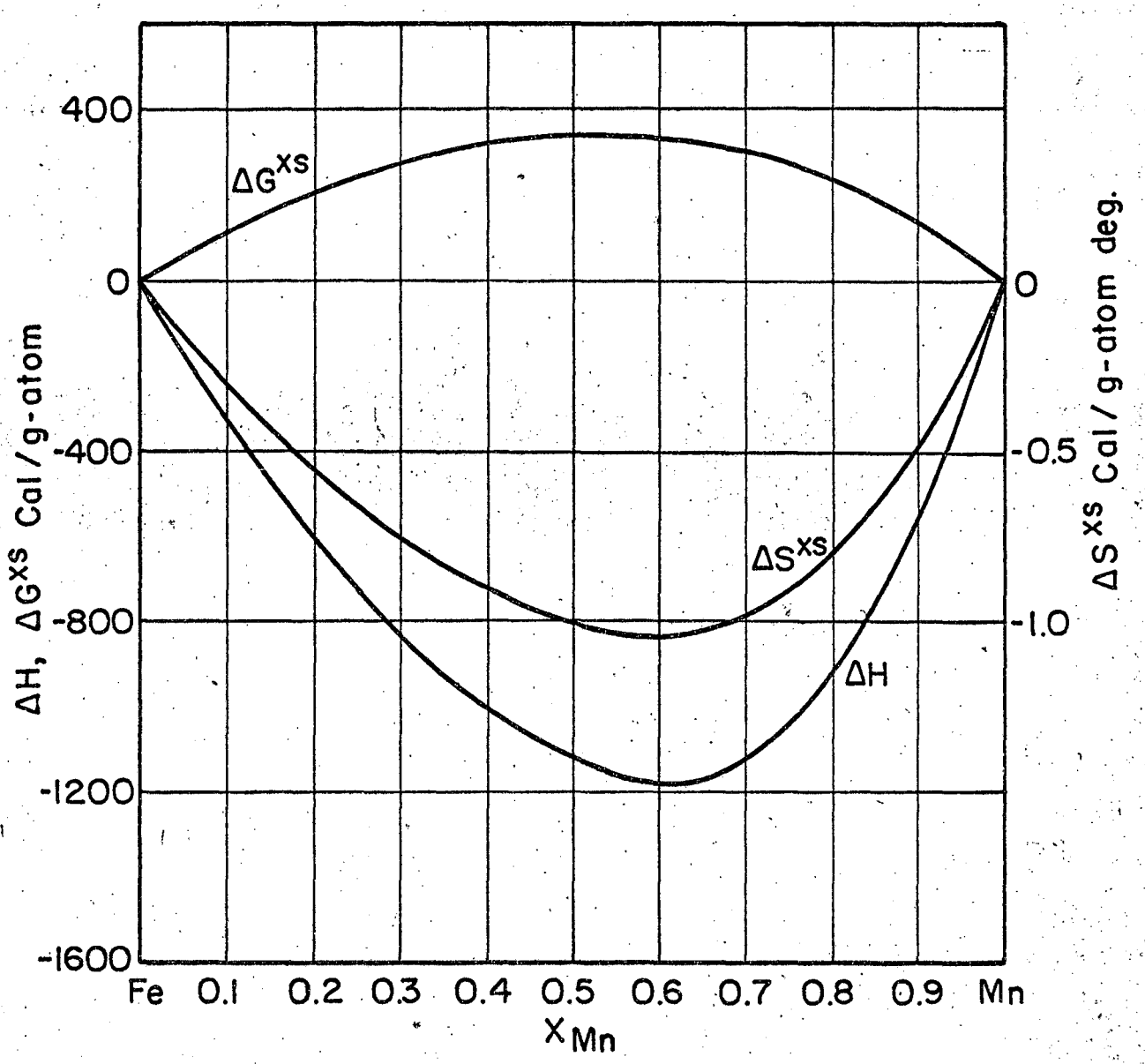

FIG. 15 INTEGRAL EXCESS QUANTITIES FOR SOLID IRON-MANGANESE ALLOYS AT 1450 °K.

VIII. DISCUSSION

The iron manganese system shows a large positive deviation from Raoult's law at all compositions (Fig. 11). This is unlike previously reported results[11] which indicated negative deviations at most concentrations with positive deviations only at high manganese concentrations. The reason for the discrepancy with the previous experimental results has been discussed as due to depletion of the surface concentration of manganese by evaporation during the experiment.

The temperature coefficients indicate negative values for $\Delta\overline{S}^{xs}_{Mn}$ at all compositions. The relative partial molar properties of iron and manganese and the integral values were obtained from Gibbs-Duhem integration and are given in Table V and Figs. 14 and 15. The data have been tabulated at 1450°K where the face-centered-cubic gamma phase is stable except near pure manganese (Fig. 4) and have been referred to γ-Fe and γ-Mn (both of which are face-centered cubic) as standard states.

The heats of formation agree well with those obtained by Kendall and Hultgren[12] from acid solution calorimetry and heat content measurements. This is strong evidence of the correctness of the present work, since experimental errors in Gibbs energy measurements are notoriously multiplied in the temperature coefficients, from which the heat of formation were calculated.

The data do not agree with vapor pressure measurements of Butler, McCabe, and Paxton,[11] who found negative deviations from Raoult's law at all concentrations. However, later work from the same laboratory,[13] on high-manganese alloys only, agree very well when activities were calculated from their previous data on pure manganese.[11] Comparative results at 1450°K are shown in Fig. 12. In this figure all measurements were translated to 1450°K using the values of $\Delta\bar{S}^{xs}_{Mn}$ determined in the present investigation. Errors in the earlier work are probably due to depletion of the manganese concentration on the surface of the sample. Butler, McCabe, and Paxton[11] were aware of this phenomenon and attempted to allow for it by extrapolating their results to zero weight loss. However, the effect is so great at the beginning that it is not surprising the extrapolation was inadequate.

Lyubimov, Granovskaya, and Berenshtein[14] studied the system by collecting the condensed vapors from evaporation from a free surface. The condensate was chemically analysed spectrographically. From chemical analyses of a series of compositions it is possible to determine activities of the components. The authors found Raoult's law was obeyed at all temperatures. Analysis of the surface of the samples showed a depletion of the manganese concentration of only two per cent.

Their results agree roughly with the Knudsen cell work (Fig. 12) but are very far from the torsion cell data. Surface depletion must be

far greater than they indicate; perhaps their surface samples were taken to a considerable depth.

An attempt was made to study surface depletion by electron probe analysis. This was done by determining the concentration profile of the sample after evaporation. Since the resolution of the probe is only one to two microns, it was very hard to detect any surface depletion from high manganese alloys, as the depletion probably occurs closer than at a distance of one micron from the evaporating surface. Only with the alloys containing 9 and 19.7 atomic percent manganese was decrease of manganese concentration beyond a distance of one micron from the surface of evaporation observed. The present study indicates about 10 to 15 percent decrease of manganese concentration at the surface, although the overall composition change calculated from the weight loss was less than one percent.

Depletion of manganese from the surface of the sample depends on the relative rates of evaporation versus diffusion. If diffusion is fast enough, the surface loss of manganese can be restored by diffusion from the interior so that the surface concentration is only slightly less than that of the sample as a whole. If diffusion is slow, the surface will quickly be depleted to a low concentration with accompanying decrease in the measured vapor pressure.

In the following discussion we shall attempt to relate surface depletion to the controllable variables temperature, are of Knudsen cell hole, and area of sample. The rate of loss of material (manganese)

from the cell is proportional to the pressure times the area of the hole. Since $P \propto e^{-(\Delta H_v/RT)}$, the

$$\text{rate of loss of Mn (grams)} \propto a e^{-(\Delta H_v/RT)} \tag{22}$$

where a = area of the effusion cell hole and ΔH_v = heat of vaporization of Mn. The significant term is the rate of loss per unit area of sample so

$$\text{rate of loss per unit area (g/cm}^2\text{)} \propto \frac{a}{A} e^{-(\Delta H_v/RT)} \tag{23}$$

where A = area of the sample.

The rate at which manganese is replenished from the interior of the sample is proportional to $Ddx/d\ell$ where D is the diffusion coefficient and $dx/d\ell$ is the concentration gradient between surface and interior. D varies with temperature so the $D \propto e^{-(Q/RT)}$ where Q is the activation energy for diffusion. Hence

$$\text{rate of replenishment } Ddx/d\ell \propto e^{-(Q/RT)} dx/d\ell \tag{24}$$

When a steady state is reached, the rate of replenishment equals the rate of loss, so from equations 23 and 24 we get

$$\frac{a}{A} e^{-(\Delta H_v/RT)} \propto Ddx/d\ell \propto e^{-(Q/RT)} dx/d\ell \tag{25}$$

and finally

$$dx/d\ell \propto \frac{a}{DA} e^{-(\Delta H_v/RT)} \propto \frac{a}{A} e^{-(\Delta H_v - Q)/RT} \tag{26}$$

The value of $dx/d\ell$ in the steady state is a measure of the magnitude of depletion. The smaller the value of $dx/d\ell$, the nearer the surface concentration of manganese is to the concentration in the interior.

It is clear that a small hole size, a, and a large area of sample, A, are favorable to bringing the steady state closer to equilibrium. The effect of temperature depends on the relative magnitudes of ΔH_v and Q. For most metals ΔH_v is much larger than Q, so that the unfavorable effect of depletion increases with temperature of measurement. For the present case, it is not so clear, since the values of Q reported by Wells and Mehl[15] for iron-manganese alloys are near the values of ΔH_v.

Depletion should be more serious at low concentrations of manganese; a one percent decrease in a ten percent Mn alloy decreases the vapor pressure by ten percent, whereas at high concentrations the decrease of vapor pressure approaches one percent for the same loss of manganese. This probably goes far to explain why the Knudsen cell method gave rather good results at high concentrations of manganese and low values at low concentrations.

Time is also a factor in the torsion method. The first and largest value of the torque, which occurs as the specimen reaches temperature, corresponds most closely with the equilibrium pressure. At low temperatures depletion takes place slowly, so that readings may be taken at a series of temperatures before depletion becomes a factor. At high temperatures depletion occurs rapidly and may

significantly reduce the measured vapor pressure before the specimen comes to temperature. This may be the explanation why the curves in Figs. 5-10 show low values at the highest temperatures.

The following precautions should be taken during the vapor pressure measurements of alloys by torsion effusion:

1. After the sample is heated, one should observe whether there is any drop in the angle of deflection with time; this will indicate the depletion of the surface concentration. A possible method for getting the equilibrium values is to observe the drop of the angle of deflection with time and extrapolate the values to zero time. However, in the present investigation this method was not successful. Since the rate of drop of the twist angle depends on the ratio of area of the hole to the area of the surface, and it was not possible to reproduce the surface area of the samples, which were in the form of fine particles, hence it was difficult to reproduce the data. Also for the lower manganese alloys the rate of drop was very rapid and the amount of deflection was very sensitive to time, hence the data scattered too much, and it was not possible to draw a smooth extrapolation curve. In order to carry out a proper extrapolation, one should also know the nature of the curve. The best results were obtained by taking the readings very rapidly to get the maximum value for the deflection at a particular temperature. However, one has to be very careful to ensure that the cell temperature is close enough to that of the dummy cell, since there is always a lag between the dummy and the torsion cell. The time

required for the torsion cell to attain the proper temperature with respect to the thermocouple located in the dummy cell was estimated from the pure manganese runs and it was found to be short, provided the torsion cell was preheated to 500 to 600°C. As the torsion cell block was made of molybdenum metal, the heat conduction was very good. A little more time than the estimated time was allowed before the measurements were made. Even so, the temperature coefficients, especially for low manganese alloys, were difficult to obtain.

IX. INTERPRETATION OF THE DATA

In the past, various models have been proposed to interpret the thermodynamic properties of metallic solid solutions in terms of the properties of their pure components. However, the lack of sufficient thermodynamic data and the complexity of the problem make it very difficult to test these theories. The excess quantities, which indicate the deviations from ideality, are the most significant thermodynamic quantities in alloy chemistry. The excess quantities obtained in this investigation are shown in Fig. 15 and Table V. The excess Gibbs energy of formation is fairly symmetrical throughout the composition range. While the excess Gibbs energies of formation are considered to be more accurate, the excess entropies can be better interpreted. The ideal entropy of mixing is

$$\Delta S^{id} = -R[x\ln x + (1-x)\ln(1-x)]$$

and the deviation from ideality can be expressed as

$$\Delta S^{xs} = \Delta S - \Delta S^{id}.$$

The large negative excess entropies in this system cannot be explained by departure from random mixing. Especially at these high temperatures any kind of ordering does not seem to be very probable.

The negative entropy, however, can be due to contributions as discussed in papers by Oriani and Murphy[16] and also by Kleppa.[17]

The difference of atomic sizes might give rise to a positive contribution to excess entropies. Since the difference of atomic sizes between iron and manganese is very small one might expect this contribution to be very small. However, the difference in electronegativity may contribute a negative entropy, but this contribution cannot be estimated in a metallic bond.

Several other major contributions to the excess entropies can be represented as follows

$$\Delta S^{xs} = \Delta S^{xs}_{vib.} + \Delta S^{xs}_{el.} + \Delta S^{xs}_{mag.} + \Delta S^{xs}_{conf.}$$

To estimate the magnitude of these contributions, however, it would be necessary to know the properties of face-centered-cubic iron and manganese. Unfortunately it is not possible to retain face-centered-cubic structures for iron at low temperatures and hence properties of this structure of iron cannot be measured. Attempts made by Weiss and Tauer[18] to estimate the properties of gamma iron are questionable since it is very difficult to separate the different contributions to the heat capacity at low temperatures. The data on face-centered-tetragonal manganese (which continuously transforms to cubic as the temperature is raised) are not very well established. The vibrational excess entropy $\Delta S^{xs}_{vib.}$ for temperatures above the Debye temperature θ can be expressed as[17]

$$\Delta S^{xs}_{vib.} \approx -3R \frac{\Delta\theta}{\theta_{alloy}}$$

where $\Delta\theta = \theta_{Fe_{1-x}Mn_x} - [x\theta_{Mn} + (1-x)\theta_{Fe}]$

and $x = x_{Mn}$

Depending on the deviation of θ for the alloy from the linear dependence on the composition, the vibrational contribution to the excess entropy will vary. A positive deviation (higher frequency of vibration) will contribute a negative excess entropy of formation. Wei, Cheng and Beck[19] have measured the low temperature heat capacity of an alloy containing 45 atomic percent manganese and 55 atomic percent iron and they report the value for θ_{alloy} to be 482°K. Estimations of θ values for iron and manganese indicate a positive deviation of θ_{alloy} from the geometric mean values for the pure components, and this will contribute to a negative $\Delta S^{xs}_{vib.}$.

The electronic excess entropy, $\Delta S^{xs}_{el.}$, term depends on the changes of electronic specific heats that occur upon alloying. If the electronic heat capacities depend linearly on the absolute temperatures ($C^E = \gamma^E T$) we have an expression for the electronic excess entropies as[17]

$$\Delta S_{el}^{xs} = \int_0^T \Delta\gamma^E T \, d\ln T = \Delta\gamma^E T$$

where $\Delta\gamma^E = \gamma^E_{Fe_{(1-x)}Mn_{(x)}} - \left[x\gamma^E_{Mn} + (1-x)\gamma^E_{Fe} \right]$.

Wei, Cheng and Beck[19] measured the low temperature heat capacity of a 45 percent atomic iron manganese alloy and found γ^E for the alloy to be 14.6×10^{-4} cal/g-atom degree. However, at present it is not possible to estimate the electronic contribution to the excess entropy since the electronic properties of face-centered cubic iron and manganese are not known.

An analysis of the contribution to the excess entropy from the magnetic properties of the alloy and its pure constituents has been made[16, 17] for silver-palladium alloys where the magnetic properties of the elements and the alloys are well known. If one of the pure components has an unpaired electron which is paired by an electron in the second component upon alloying, this will contribute to the excess entropy depending on the degree of order in the orientation of the localized spin.

Although attempts have been made to determine or estimate the magnetic properties of gamma iron[18] and gamma manganese[20] and of a few iron-manganese alloys[21] at present it is very difficult to draw any conclusion.

X. CONCLUSION

The activities of manganese and its temperature coefficients between 1240° and 1510°K in the iron-manganese system have been measured by Knudsen and torsion effusion techniques. The heats of formation calculated from the present data at 1450° agree fairly well with the values obtained previously by acid solution calorimetry and heat content measurements by Kendall and Hultgren.[12] The relative partial excess Gibbs energies for the manganese component obtained by this investigation are 100 to 700 cal/gram atom more positive than the values obtained by Butler, McCabe and Paxton[11] and Lyubimov et al.[14] This discrepancy is attributed to the depletion of surface concentration of manganese in the alloy in the previous investigations. The present data agree very well with Smith, Paxton and McCabe.[13]

A severe surface depletion of manganese was observed during the course of the experiment for alloys containing less than 40 atomic percent manganese. The increase of rate of diffusion of manganese by 125 percent when the manganese concentration in the alloy was increased from 4 to 60 atomic percent as observed by Well and Mehl[15] tends to confirm the present observation that the surface depletion becomes more significant for lower manganese concentrations. A few possible solutions to overcome the depletion of the vaporizing component at the surface of the alloy have been suggested. An attempt has been made to explain the observed rather large negative excess entropies of formation in terms of the properties of the pure components.

ACKNOWLEDGEMENTS

I am pleased to express my gratitude and indebtedness to:

Professor Ralph Hultgren, for his advice and encouragement extended throughout this work.

My friend, Mr. Raymond Orr, for helping me in the experimental work and for his invaluable contributions to the interpretation of the experimental results.

Professor S. F. Ravitz and Professor O. Redlich, for many interesting discussions.

Mr. D. T. Hawkins, for helping me with the analyses of the alloys.

Mrs. G. Buechley for typing the manuscript.

This work was performed under the auspices of the United States Atomic Energy Commission.

TABLES IIIa through IIIf and IVa through IVℓ

Assumed values for pure manganese used in calculation (see Reference 10)

$\Delta H_{v,298}$ = 67060 cal/g-atom

$\Delta S_{Tr}^{\gamma-\delta}$ = 0.30 cal/g-atom deg.

$T_{Tr}^{\gamma-\delta}$ = 1410°K

TABLE IIIa

Calibration of the Cell Assembly with Pure Manganese Sample

Hole Area~0.0015 cm^2 Ribbon No. 1

T°K	Deflection Angle, deg.	P^*_{Mn}, 10^{-5} atm	Factor 10^{-6} atm/deg.	P^{**}_{Mn}, 10^{-5} atm	ΔH^v_{298}, cal
1311	3.00	6.493	21.64	6.510	67053
1332	4.40	9.534	21.67	9.548	67050
1346	5.50	12.15	22.09	11.94	67113
1356	6.70	14.53	21.69	14.54	67056
1368	8.20	17.79	21.70	17.79	67057
1381	10.05	22.08	21.97	21.81	67094
1402	14.30	31.05	21.71	31.03	67048
1414	17.50	37.52	21.44	37.98	67025
1430	22.15	48.02	21.68	48.07	67071
1445	27.60	60.13	21.79	59.89	67086
1457	33.10	71.80	21.69	71.83	67058
1471	40.40	87.74	21.72	87.67	67060
1481	47.75	101.7	21.28	103.6	66996

Average Factor: 1° deflection = 21.70×10^{-6} atm

P^*_{Mn} taken from ref[10]

P^{**}_{Mn} calculated from the average factor.

TABLE IIIb

Calibration of the Cell Assembly with Pure Manganese Sample

Hole Area~0.0015 cm^2 Circular wire 2 mil diameter

T°K	Deflection Angle, deg.	P^*_{Mn}, 10^{-5} atm	Factor 10^{-6} atm/deg.	P^{**}_{Mn}, 10^{-5} atm	ΔH^v_{298}, cal
1314	1.65	6.955	42.15	6.963	67023
1336	2.40	10.19	42.45	10.13	67104
1361	3.75	15.82	42.19	15.83	67054
1381	5.25	22.08	42.06	22.16	67040
1404	7.60	32.12	42.26	32.07	67079
1428	11.00	46.42	42.20	46.42	67063
1454	16.30	68.79	42.20	68.79	67055
1481	24.10	101.6	42.16	101.7	67042
1453	16.05	67.67	42.16	67.73	67040
1428	11.00	46.42	42.20	46.42	67063
1358	3.55	14.99	42.23	14.98	67085
1313	1.60	6.752	42.20	6.752	67067

Average Factor: 1° deflection = 42.20×10^{-6} atm

P^*_{Mn} taken from ref[10]

P^{**}_{Mn} calculated from the average factor.

TABLE IIIc

Calibration of the Cell Assembly with Pure Manganese Sample

Hole Area~0.0028 cm^2 Ribbon No. 1

T°K	Deflection Angle, deg.	P^*_{Mn}, 10^{-5} atm	Factor 10^{-6} atm/deg.	P^{**}_{Mn}, 10^{-5} atm	ΔH^v_{298}, cal
1313	5.60	6.742	12.04	6.854	67021
1335	8.00	10.04	12.55	9.792	67157
1359	12.45	15.23	12.23	15.24	67061
1377	17.00	20.67	12.16	20.81	67042
1405	27.20	32.61	11.99	33.29	67009
1430	38.00	48.04	12.64	46.51	67150
1455	57.80	69.91	12.10	70.75	67039
1289	3.50	4.312	12.32	4.284	67076
1336	8.40	10.22	12.17	10.28	67052
1350	10.65	13.06	12.26	13.04	67062
1366	14.05	17.19	12.23	17.20	67051
1377	16.65	20.67	12.41	20.38	67099
1391	21.25	26.07	12.27	26.01	67065
1405	26.60	32.61	12.26	32.56	67070
1420	32.40	41.19	12.33	39.66	67173
1437	44.20	53.32	12.06	54.10	67019
1451	53.60	65.57	12.23	65.61	67058
1467	68.50	82.82	12.09	83.84	67023

Average Factor: 1° deflection = 12.24×10^{-6} atm

P^*_{Mn} taken from ref[10]

P^{**}_{Mn} calculated from the average factor.

TABLE IIId

Calibration of the Cell Assembly with Pure Manganese Sample

Hole Area ~ 0.0028 cm^2 Circular wire 2 mil diameter

T°K	Deflection Angle, deg.	P^*_{Mn}, 10^{-5} atm	Factor 10^{-6} atm. deg.	P^{**}_{Mn}, 10^{-5} atm	ΔH^v_{298}, cal
1311	3.40	6.493	19.09	6.338	67122
1322	4.30	7.964	18.52	8.015	67042
1342	6.00	11.36	18.93	11.18	67102
1360	8.35	15.53	18.60	15.56	67054
1367	9.35	17.46	18.67	17.43	67064
1391	14.20	26.06	18.35	26.47	67017
1414	20.10	37.52	18.67	37.47	67063
1431	27.60	50.18	18.18	51.45	66911
1445	32.25	60.13	18.64	60.11	67060
1464	42.80	79.40	18.55	79.78	67046
1476	49.20	90.58	18.41	91.71	67142
1443	30.50	58.36	19.13	56.85	67128
1420	22.15	41.19	18.60	41.29	67089
1391	13.75	26.06	18.95	25.63	67105
1361	8.80	15.82	17.97	16.40	66962
1324	4.40	8.232	18.71	8.202	67070
1312	3.50	6.625	18.93	6.524	67098

Average Factor: 1° deflection = 18.64×10^{-6} atm

P^*_{Mn} taken from ref[10]

P^{**}_{Mn} calculated from the average factor.

TABLE IIIe

Calibration of the Cell Assembly with Pure Manganese Sample

Hole Area~0.0028 cm^2 Ribbon No. 2

T°K	Deflection Angle, deg.	P^*_{Mn}, 10^{-5} atm	Factor 10^{-6} atm/deg.	P^{**}_{Mn}, 10^{-5} atm	ΔH^v_{298}, cal
1315	5.60	7.156	12.78	7.168	66992
1332	7.60	9.677	12.73	9.728	67121
1356	11.10	14.53	13.09	14.21	67115
1373	15.20	19.35	12.73	19.46	67044
1394	21.25	27.32	12.86	27.20	67072
1416	31.60	38.80	12.28	40.45	66928
1432	39.20	50.18	12.80	50.18	67016
1453	52.00	67.67	13.01	66.56	67109
1468	66.90	84.12	12.57	85.63	66985
1480	80.80	99.82	12.35	103.4	66927
1449	49.80	63.82	12.82	63.74	67060
1420	31.40	41.19	13.12	40.19	67122
1381	17.35	22.08	12.73	22.21	67043
1354	10.80	14.05	13.01	13.82	67091
1322	6.25	7.964	12.74	8.000	67074
1267	2.10	2.770	13.19	2.688	67167

Average Factor: 1° deflection = 12.80×10^{-6} atm

P^*_{Mn} taken from ref[10]

P^{**}_{Mn} calculated from the average factor.

TABLE IIIf

Calibration of the Cell Assembly with Pure Manganese Sample

Hole Area~0.010 cm^2 Circular wire 2 mil diameter

T°K	Deflection Angle, deg.	P^*_{Mn}, 10^{-5} atm	Factor 10^{-6} atm/deg.	P^{**}_{Mn}, 10^{-5} atm	ΔH^v_{298}, cal
1246	3.30	1.834	5.56	1.861	67028
1267	4.90	2.770	5.65	2.764	67098
1289	7.50	4.312	5.75	4.230	67109
1313	12.20	6.742	5.51	6.881	67010
1337	18.40	10.37	5.64	10.38	67062
1359	27.05	15.23	5.63	15.26	67070
1382	39.45	22.48	5.70	22.25	67088
1406	58.65	33.08	5.64	33.08	67060
1432	90.00	50.18	5.58	50.76	66980
1454	123.00	68.79	5.59	69.37	67035
1482	184.10	102.7	5.58	103.8	67036
1455	122.00	69.91	5.73	68.81	67090
1406	58.85	33.09	5.62	33.19	67050
1359	26.60	15.23	5.72	15.00	67117
1315	12.85	7.155	5.56	7.247	66963
1267	4.80	2.770	5.77	2.707	67151

Average Factor: 1° deflection = 5.64×10^{-6} atm

P^*_{Mn} taken from ref[10]

P^{**}_{Mn} calculated from the average factor.

TABLE IVa

Manganese Vapor Pressure by Torsion Effusion Technique

$x_{Mn} = 0.09$

T°K	Deflection Angle, deg.	P, 10^{-5} atm	a_{Mn}	$\Delta\bar{G}^{xs}_{Mn}$ cal/g-atom.
Hole Area~0.0015 cm^2; Ribbon No. 1; 1° deflection = 21.70 x 10^{-6} atm.				
1409	2.00	4.340	0.125	912
1458	4.40	9.548	0.130	1064
1485	6.25	13.56	0.125	971
1512	8.55	18.55	0.118	810
Hole Area~0.0028 cm^2; Ribbon No. 1; 1° deflection = 12.24 x 10^{-6} atm.				
1359	1.50	1.836	0.121	779
1383	2.30	2.815	0.123	853
1406	3.35	4.100	0.123	888
1432	4.95	6.059	0.122	867
1456	7.35	8.996	0.127	984
1484	10.15	12.42	0.117	757
1509	13.45	16.46	0.113	679
Hole Area~0.01 cm^2; 2 mil diameter wire; 1° deflection = 5.64 x 10^{-6} atm.				
1312	1.35	0.7614	0.115	633
1334	2.10	1.184	0.119	730
1357	3.15	1.777	0.122	777
1382	4.80	2.707	0.120	793
1406	7.05	3.976	0.120	802
1428*	9.50	5.358	0.115	692
1313*	1.45	0.8178	0.119	716
1359*	3.30	1.861	0.122	816
1407*	7.35	4.145	0.123	870

Selected $\Delta\bar{S}^{xs}_{Mn}$ = -2.80 cal/g-atom. deg.

* short runs

All values are referred to gamma Mn as the standard state.

TABLE IVb

Manganese Vapor Pressure by Torsion Effusion Technique

$x_{Mn} = 0.197$

T°K	Deflection Angle, deg.	P, 10^{-5} atm	a_{Mn}	$\Delta\bar{G}^{xs}_{Mn}$ cal/g-atom.
Hole Area~0.0015 cm^2; Ribbon No. 1; 1° deflection = 21.70 x 10^{-6} atm.				
1334	1.15	2.496	0.251	639
1356	1.65	3.581	0.241	539
1382	2.60	5.642	0.251	668
1405	3.90	8.465	0.260	772
1431	5.85	12.69	0.259	784
1456	8.35	18.12	0.255	752
1482	12.00	26.04	0.252	725
1508	16.95	36.78	0.249	702
Hole Area~0.0028 cm^2; Ribbon No. 1; 1° deflection = 12.24 x 10^{-6} atm.				
1312	1.30	1.591	0.241	521
1335	2.05	2.509	0.247	602
1359	3.10	3.794	0.249	634
1377*	4.25	5.202	0.252	673
1406*	6.95	8.507	0.257	747
1430*	10.00	12.24	0.255	731
Hole Area~0.01 cm^2; 2 mil diameter wire; 1° deflection = 5.64 x 10^{-6} atm.				
1290	1.90	1.072	0.239	496
1313	2.95	1.664	0.242	540
1337	4.60	2.594	0.247	606
1356	6.45	3.638	0.251	653
1380	9.85	5.555	0.256	721
1407*	14.95	8.432	0.251	676
1359*	6.65	3.751	0.246	603
1406*	15.30	8.629	0.261	787

Selected $\Delta\bar{S}^{xs}_{Mn}$ = 2.42 cal/g-atom. deg.

* short runs

All values are referred to gamma Mn as the standard state

TABLE IVc

Manganese Vapor Pressure by Torsion Effusion Technique

$x_{Mn} = 0.253$

T°K	Deflection Angle, deg.	P, 10^{-5} atm	a_{Mn}	$\Delta\overline{G}^{xs}_{Mn}$ cal/g-atom.
Hole Area~0.0015 cm^2; Ribbon No. 1; 1° deflection = 21.70 x 10^{-6} atm.				
1336	1.45	3.147	0.306	500
1359	2.20	4.774	0.313	573
1383	3.40	7.378	0.323	666
1406	4.95	10.74	0.325	695
1431	7.15	15.52	0.317	642
1456	10.00	21.70	0.306	547
Hole Area~0.0028 cm^2; Ribbon No. 1; 1° deflection = 12.24 x 10^{-6} atm.				
1288	1.05	1.285	0.300	404
1312	1.65	2.020	0.304	476
1337	2.65	3.244	0.309	530
1357	3.80	4.651	0.315	590
1382	5.80	7.099	0.316	609
1405	8.50	10.40	0.319	645
1430	12.55	15.36	0.319	660
1315*	1.75	2.142	0.301	448
1359*	3.95	4.835	0.317	609
1406*	8.70	10.65	0.322	672
Hole Area~0.01 cm^2; 2 mil diameter wire; 1° deflection = 5.64 x 10^{-6} atm.				
1290	2.35	1.325	0.295	394
1314	3.75	2.115	0.303	466
1337	5.75	3.243	0.309	530
1359	8.40	4.738	0.311	554
1381	11.95	6.740	0.305	514
1405	17.45	9.842	0.282	306

Selected $\Delta\overline{S}^{xs}_{Mn} = -2.22$ cal/g-atom. deg.

* short runs

All values are referred to gamma Mn as the standard state

TABLE IVd

Manganese Vapor Pressure by Torsion Effusion Technique

$x_{Mn} = 0.318$

T°K	Deflection Angle, deg.	P, 10^{-5} atm	a_{Mn}	$\Delta\bar{G}^{xs}_{Mn}$ cal/g-atom.
Hole Area~0.0015 cm^2; Ribbon No. 1; 1° deflection = 21.70 x 10^{-6} atm.				
1313	1.20	2.604	0.378	455
1331	1.60	3.472	0.367	382
1356	2.50	5.425	0.374	442
1380	3.85	8.355	0.385	529
1403	5.45	11.83	0.387	550
1428	8.40	18.23	0.392	597
1448	11.45	24.85	0.394	623
1477	17.50	37.98	0.394	634
1506	25.90	56.20	0.387	598
Hole Area~0.0028 cm^2; Ribbon No. 2; 1° deflection = 12.80 x 10^{-6} atm.				
1312	1.90	2.432	0.367	380
1335	2.90	3.712	0.359	327
1358	4.45	5.696	0.381	488
1381	6.65	8.512	0.386	533
1405	9.85	12.61	0.387	550
1429	14.40	18.43	0.389	577
1455	21.25	27.20	0.396	641
1482	31.05	39.74	0.384	560
Hole Area~0.01 cm^2; 2 mil diameter wire; 1° deflection = 5.64 x 10^{-6} atm.				
1289	2.85	1.607	0.365	358
1315	4.65	2.623	0.368	385
1338	7.10	4.004	0.375	439
1359	10.25	5.781	0.379	480
1383	15.45	8.714	0.381	501
1406	22.45	12.66	0.383	522
1430	32.00	18.05	0.375	475
1457	48.05	27.10	0.371	487

Selected $\Delta\bar{S}^{xs}_{Mn} = -1.99$ cal/g-atom. deg.

All values are referred to gamma Mn as the standard state

TABLE IVe

Manganese Vapor Pressure by Torsion Effusion Technique

$x_{Mn} = 0.349$

T°K	Deflection Angle, deg.	P, 10^{-5} atm	a_{Mn}	$\Delta\bar{G}^{xs}_{Mn}$ cal/g-atom.
Hole Area~0.0015 cm^2; Ribbon No. 1; 1° deflection = 21.70 x 10^{-6} atm.				
1335	1.90	4.123	0.406	412
1361	3.00	6.510	0.411	452
1375	3.80	8.246	0.413	473
1404	6.20	13.45	0.419	519
1428	9.10	19.75	0.425	567
1459	14.55	31.57	0.426	590
1382*	4.35	9.440	0.420	519
1431*	9.70	21.05	0.430	607
1456*	14.05	30.49	0.430	613
Hole Area~0.0028 cm^2; Ribbon No. 1; 1° deflection = 12.24 x 10^{-6} atm.				
1313	2.25	2.754	0.400	365
1337	3.45	4.223	0.403	389
1359	5.10	6.242	0.410	442
1382	7.60	9.302	0.414	480
1406	11.35	13.89	0.420	529
1432	17.00	20.81	0.420	539
1406*	11.30	13.83	0.419	517
1455*	24.20	29.62	0.421	574
Hole Area~0.01 cm^2; 2 mil diameter wire; 1° deflection = 5.64 x 10^{-6} atm.				
1289	3.10	1.748	0.397	342
1312	4.65	2.623	0.396	340
1335	7.30	4.117	0.406	408
1358	10.85	6.119	0.409	437
1381	16.10	9.080	0.411	461
1406	24.35	13.73	0.415	497
1430	35.40	19.96	0.413	439
1380*	16.05	9.052	0.417	500
1407*	24.70	13.93	0.414	489

Selected $\Delta\bar{S}^{xs}_{Mn} = -1.88$ cal/g-atom. deg.

* short runs

All values are referred to gamma Mn as the standard state

TABLE IVf

Manganese Vapor Pressure by Torsion Effusion Technique

$x_{Mn} = 0.402$

T°K	Deflection Angle, deg.	P, 10^{-5} atm	a_{Mn}	$\Delta\bar{G}^{xs}_{Mn}$ cal/g-atom.
Hole Area~0.0015 cm^2; 2 mil diameter wire; 1° deflection = 42.20 x 10^{-6} atm				
1336	1.15	4.853	0.463	377
1380	2.40	10.13	0.471	432
1408	3.80	16.04	0.469	430
1432	5.60	23.63	0.479	501
1457	8.15	34.39	0.472	503
1480	11.25	47.48	0.474	488
Hole Area~0.0028 cm^2; Ribbon No. 1; 1° deflection = 12.24 x 10^{-6} atm.				
1290	1.60	1.958	0.438	221
1315	2.60	3.182	0.448	286
1336	3.80	4.651	0.454	322
1361	5.95	7.283	0.455	374
1381	8.40	10.28	0.467	415
1404	12.35	15.12	0.473	453
1428	18.10	22.155	0.486	539
1454	26.70	32.68	0.475	484
1481	38.75	47.43	0.457	436
Hole Area~0.01 cm^2; 2 mil diameter wire; 1° deflection = 5.64 x 10^{-6} atm.				
1245	1.40	0.7896	0.430	163
1266	2.20	1.261	0.442	241
1288	3.40	1.918	0.445	258
1313	5.45	3.704	0.448	285
1334	8.00	4.512	0.455	327
1358	12.20	6.881	0.462	374
1382	18.45	10.41	0.459	402
1406	27.50	15.51	0.471	443
1430	39.90	22.50	0.470	444
1456	58.55	33.02	0.467	436
1482	83.60	47.15	0.458	385

Selected $\Delta\bar{S}^{xs}_{Mn} = -1.70$ cal/g-atom. deg.

All values are referred to gamma Mn as the standard state

TABLE IVg

Manganese Vapor Pressure by Torsion Effusion Technique

$x_{Mn} = 0.452$

T°K	Deflection Angle, deg.	P, 10^{-5} atm	a_{Mn}	$\Delta\bar{G}^{xs}_{Mn}$ cal/g-atom.
Hole Area~0.0015 cm^2; Ribbon No 1; 1° deflection = 21.70 x 10^{-6} atm.				
1315	1.60	3.472	0.481	162
1338	2.45	5.317	0.497	254
1359	3.55	7.704	0.506	301
1383	5.40	11.72	0.506	344
1408	8.15	17.69	0.517	375
1433	12.10	26.26	0.522	408
1457	17.60	38.19	0.530	458
1483	25.50	55.34	0.535	496
1509	36.65	79.53	0.527	460
Hole Area~0.0028 cm^2; 2 mil wire; 1° deflection = 18.64 x 10^{-6} atm.				
1312	1.75	3.262	0.493	226
1337	2.80	5.219	0.498	254
1357	4.00	7.456	0.505	297
1382	6.15	11.46	0.504	332
1405	9.00	16.78	0.514	361
1430	13.45	25.07	0.515	405
1456	20.10	37.47	0.527	444
1483	29.90	55.73	0.542	490
1509	42.20	78.66	0.522	429
1407*	9.40	17.52	0.511	395
1456*	20.15	37.56	0.529	455

TABLE IVg (continued)

Manganese Vapor Pressure by Torsion Effusion Technique

$x_{Mn} = 0.452$

Hole Area~0.01 cm^2; 2 mil diameter wire; 1° deflection = 5.64 x 10^{-6} atm.				
T°K	Deflection Angle, deg.	P, 10^{-5} atm	a_{Mn}	$\Delta\bar{G}^{xs}_{Mn}$ cal/g-atom.
1268	2.50	1.410	0.480	150
1289	3.80	2.143	0.487	191
1313	6.00	3.380	0.491	217
1335	8.90	5.020	0.494	237
1380	19.55	11.03	0.500	340
1406	30.20	17.03	0.515	364
1430	44.45	25.07	0.523	415
1456	65.25	36.80	0.519	398
1481	94.20	53.13	0.521	415
1506	132.40	74.67	0.515	392
1266	2.35	1.325	0.470	99
1289	3.85	2.171	0.493	224
1311	5.70	3.215	0.495	239
1333	8.50	4.794	0.490	215
1359	13.80	7.783	0.510	328
1382	20.05	11.31	0.503	296
1429	44.45	25.07	0.530	450
1443	55.20	31.13	0.531	464

Selected $\Delta\bar{S}^{xs}_{Mn} = -1.52$ cal/g-atom deg.

* short runs

All values are referred to gamma Mn as the standard state

TABLE IVh

Manganese Vapor Pressure by Torsion Effusion Technique

$x_{Mn} = 0.499$

T°K	Deflection Angle, deg.	P, 10^{-5} atm	a_{Mn}	$\Delta\bar{G}^{xs}_{Mn}$ cal/g-atom.
Hole Area ~ 0.0015 cm^2; Ribbon No. 1; 1° deflection = 21.70 x 10^{-6} atm.				
1313	1.70	3.689	0.536	184
1331	2.35	5.099	0.540	202
1356	3.65	7.921	0.547	243
1380	5.55	12.04	0.556	294
1406	8.60	18.66	0.564	342
1428	12.10	26.26	0.565	348
1448	16.60	36.02	0.572	389
1479	26.35	57.18	0.578	429
1506	38.20	82.89	0.572	408
1517	44.85	97.33	0.575	423
Hole Area ~ 0.0028 cm^2; Ribbon No. 2; 1° deflection = 12.80 x 10^{-6} atm.				
1315	3.20	4.096	0.562	308
1336	4.35	5.568	0.541	212
1359	6.55	8.384	0.545	235
1382	9.45	12.10	0.544	208
1406	14.45	18.50	0.560	319
1430	21.40	27.39	0.570	375
1457	31.85	40.77	0.565	358
1482	46.35	59.33	0.574	411
1509	67.20	86.02	0.571	399

TABLE IVh (continued)

$x_{Mn} = 0.499$

Hole Area~0.01 cm^2; 2 mil diameter wire; 1° deflection = 5.64 x 10^{-6} atm.				
T°K	Deflection Angle, deg.	P, 10^{-5} atm	a_{Mn}	$\Delta\bar{G}^{xs}_{Mn}$ cal/g-atom
1268	2.75	1.551	0.528	140
1287	4.00	2.256	0.532	161
1311	6.15	3.469	0.535	178
1336	9.85	5.555	0.539	205
1358	14.65	8.263	0.552	271
1382	22.20	12.52	0.557	302
1406	33.15	18.70	0.566	349
1428	46.90	26.45	0.569	368
1456	70.05	39.51	0.557	315
1481	100.10	56.46	0.553	300

Selected $\Delta\bar{S}^{xs}_{Mn}$ = -1.35 cal/g-atom. deg.

All values are referred to gamma Mn as the standard state

TABLE IVi

Manganese Vapor Pressure by Torsion Effusion Technique

$x_{Mn} = 0.548$

T°K	Deflection Angle, deg.	P, 10^{-5} atm	a_{Mn}	$\Delta\bar{G}^{xs}$ cal/g-atom.
Hole Area~0.0015 cm^2; Ribbon No. 1; 1° deflection = 21.70 x 10^{-6} atm.				
1312	1.80	3.906	0.592	200
1336	2.75	5.968	0.580	147
1358	4.05	8.789	0.587	183
1381	6.10	13.24	0.600	246
1405	9.00	19.53	0.599	247
1429	13.25	28.75	0.600	288
1456	19.95	43.29	0.610	307
1482	29.60	64.23	0.621	367
1509	43.05	93.42	0.618	362
Hole Area~0.0028 cm^2; Ribbon No. 1; deflection = 12.24 x 10^{-6} atm.				
1313	3.25	3.978	0.579	142
1336	4.90	5.998	0.582	160
1358	7.20	8.813	0.588	191
1382	10.95	13.40	0.597	231
1406	16.25	19.89	0.606	258
1428	23.00	28.15	0.605	280
1456	35.65	43.64	0.615	331
1481	51.00	62.42	0.611	318
1506	72.00	88.13	0.608	308
Hole Area~0.01 cm^2; 2 mil diameter wire; 1° deflection = 5.64 x 10^{-6} atm.				
1267	2.90	1.636	0.568	90
1290	4.55	2.566	0.572	107
1311	6.65	3.751	0.578	135
1336	10.65	6.007	0.583	164
1360	16.25	9.165	0.592	199
1381	23.35	13.17	0.585	204
1405	34.70	19.57	0.600	252
1430	51.20	28.88	0.599	250
1453	74.35	41.93	0.617	338
1482	108.70	61.31	0.592	230

Selected $\Delta\bar{S}^{xs}_{Mn} = -1.18$ cal/g-atom. deg.

All values are referred to gamma Mn as the standard state

TABLE IVj

Manganese Vapor Pressure by Torsion Effusion Technique

$x_{Mn} = 0.597$

T°K	Deflection Angle, deg.	P, 10^{-5} atm	a_{Mn}	$\Delta\bar{G}^{xs}_{Mn}$ cal/g-atom.
Hole Area~0.0015 cm^2; Ribbon No. 1; 1° deflection = 21.70 x 10^{-6} atm.				
1313	2.00	4.34	0.630	148
1333	2.90	6.293	0.644	200
1358	4.45	9.657	0.645	208
1380	6.40	13.89	0.644	210
1404	9.55	20.72	0.645	216
1430	14.35	31.14	0.648	230
1454	20.75	45.03	0.652	254
1482	31.20	67.70	0.655	271
1508	44.50	96.56	0.653	268
Hole Area~0.0028 cm^2; Ribbon No. 1; 1° deflection = 12.24 x 10^{6} atm.				
1313	3.55	4.345	0.632	149
1331	4.90	5.998	0.634	158
1356	7.55	9.241	0.637	175
1380	11.25	13.77	0.635	171
1403	16.35	20.01	0.654	254
1428	24.75	30.29	0.651	245
1448	33.55	41.07	0.652	252
1490	62.15	76.07	0.655	275
1506	77.30	94.62	0.657	269
Hole Area~0.01 cm^2; 2 mil diameter wire; 1° deflection = 5.64 x 10^{-6} atm.				
1268	3.25	1.833	0.623	109
1290	5.00	2.820	0.629	130
1337	11.85	6.683	0.637	171
1382	25.60	14.38	0.640	191
1432	57.00	32.15	0.650	240
1454	79.95	45.09	0.653	258
1482	119.50	67.40	0.652	259
1508	170.20	95.99	0.649	251

Selected $\Delta\bar{S}^{xs}_{Mn}$ = -1.00 cal/g-atom. deg.

All values are referred to gamma Mn as the standard state

TABLE IVk

Manganese Vapor Pressure by Torsion Effusion Technique

$x_{Mn} = 0.700$

T°K	Deflection Angle, deg.	P, 10^{-5} atm	a_{Mn}	$\Delta\bar{G}^{xs}_{Mn}$ cal/g-atom.
Hole Area ~ 0.0015 cm^2; Ribbon No. 1; 1° deflection = 42.20 x 10^{-6} atm.				
1336	1.80	7.596	0.738	140
1381	3.85	16.25	0.736	137
1406	5.80	24.48	0.740	155
1432	8.75	36.93	0.745	179
1455	12.30	51.91	0.744	173
1482	18.30	77.23	0.747	189
1509	26.90	113.5	0.757	215
Hole Area ~ 0.0028 cm^2; Ribbon No. 2; 1° deflection = 12.80 x 10^{-6} atm.				
1267	1.60	2.048	0.711	41
1291	2.60	3.328	0.727	95
1310	3.65	4.672	0.731	111
1337	6.00	7.680	0.732	118
1360	8.90	11.39	0.733	127
1378	12.10	15.49	0.740	139
1403	17.65	22.59	0.743	149
1431	28.40	36.35	0.745	173
1456	41.40	52.99	0.747	186
1484	62.30	79.74	0.750	201
1501	78.95	101.1	0.748	198
Hole Area ~ 0.01 cm^2; 2 mil diameter wire; 1° deflection = 5.64 x 10^{-6} atm.				
1267	3.70	2.087	0.725	88
1289	5.70	3.215	0.733	115
1313	8.90	5.020	0.730	105
1337	13.65	7.699	0.733	124
1359	19.80	11.17	0.733	124
1382	29.35	16.55	0.736	140
1406	43.40	24.48	0.740	156
1432	65.30	36.83	0.743	172
1454	90.50	51.04	0.740	159
1482	135.60	76.48	0.740	162

Selected $\Delta\bar{S}^{xs}_{Mn}$ = -0.64 cal/g-atom. deg.

All values are referred to gamma Mn as the standard state

TABLE IVℓ

Manganese Vapor Pressure by Torsion Effusion Technique

$x_{Mn} = 0.802$

T°K	Deflection Angle, deg.	P, 10^{-5} atm	a_{Mn}	$\Delta\bar{G}^{xs}_{Mn}$ cal/g atom.
Hole Area~0.0015 cm^2; 2 mil diameter wire; 1° deflection = 42.20 x 10^{-6} atm.				
1361	3.05	12.87	0.813	37
1382	4.35	18.36	0.817	54
1405	6.30	26.59	0.816	50
1455	13.50	56.99	0.816	52
1482	20.15	85.03	0.822	76
1503	27.00	113.9	0.819	64
1479**	19.25	81.24	0.821	70
1457**	14.05	59.28	0.822	74
Hole Area~0.01 cm^2; 2 mil diameter wire; 1° deflection = 5.64 x 10^{-6} atm.				
1267	4.15	2.341	0.814	38
1289	6.35	3.581	0.814	40
1313	9.95	5.612	0.815	45
1337	15.15	8.545	0.813	38
1359	22.05	12.44	0.819	50
1382	32.50	18.33	0.818	49
1406	47.85	26.99	0.816	52
1432	71.80	40.50	0.819	61
1454	101.00	56.96	0.824	82
1482	150.80	85.05	0.822	77
1455**	100.90	56.91	0.814	45
1406**	47.80	26.96	0.816	49
1359**	22.10	12.46	0.819	54

Selected $\Delta\bar{S}^{xs}_{Mn} = -0.314$ cal/g-atom. deg.

** cooling runs

All values are referred to gamma Mn as the standard state

TABLE V

Integral Quantities for Fe-Mn Alloys at 1450° K

$$(1-x)Fe_{(\gamma)} + xMn_{(\gamma)} = Fe_{(1-x)}Mn_{x(\gamma)}$$

x_{Mn}	Phase	ΔG	ΔH	ΔS	ΔG^{xs}	ΔS^{xs}
0	γ	0	0	0	0	0
0.1		-825	-316	0.351	112	-0.295
0.2		-1240	-592	0.447	202	-0.548
0.3		-1488	-825	0.457	272	-0.756
0.4		-1621	-1009	0.422	318	-0.915
0.5		-1659	-1122	0.370	338	-1.007
		(±70)	(±400)	(±0.25)	(±70)	(±.025)
0.6		-1607	-1183	0.293	332	-1.044
0.7		-1457	-1121	0.232	303	-0.982
0.8		-1200	-926	0.189	241	-0.805
0.9		-794	-564	0.158	142	-0.487
1.0	δ	0	0	0	0	0

TABLE Va

Partial Molar Quantities for Fe-Mn Alloys at 1450° K

A. Mn Component $Mn_{(\gamma)(s)} = Mn\ (\text{in alloy})_{(\gamma)(s)}$

x_{Mn}	Phase	a_{Mn}	γ_{Mn}	$\Delta\bar{G}_{Mn}$	$\Delta\bar{G}^{xs}_{Mn}$	$\Delta\bar{H}_{Mn}$	$\Delta\bar{S}_{Mn}$	$\Delta\bar{S}^{xs}_{Mn}$
0	γ	0.000	1.524	$-\infty$	1215	-3353	∞	-3.150
0.1		0.143	1.428	-5608	1027	-2966	1.822	-2.754
0.2		0.268	1.341	-3791	846	-2634	0.798	-2.400
0.3		0.388	1.294	-2792	676	-2294	0.344	-2.048
0.4		0.468	1.170	-2121	520	-1954	0.115	-1.706
0.5		0.570	1.141	-1617	381	-1577	0.027	-1.350
		(± 0.014)	(± 0.027)	(±70)	(± 70)	(± 400)	(±0.25)	(±0.25)
0.6		0.658	1.097	-1206	265	-1171	0.025	-0.990
0.7		0.742	1.060	-862	166	-755	0.074	-0.635
0.8		0.823	1.029	-561	82	-381	0.124	-0.319
0.9		0.907	1.008	-281	23	-108	0.119	-0.090
1.0	δ	1.000	1.000	0	0	0	0	0

B. Fe Component $Fe_{(\gamma)(s)} = Fe\ \text{in alloy}_{(\gamma)(s)}$

x_{Fe}	Phase	a_{Fe}	γ_{Fe}	$\Delta\bar{G}_{Fe}$	$\Delta\bar{G}^{xs}_{Fe}$	$\Delta\bar{H}_{Fe}$	$\Delta\bar{S}_{Fe}$	$\Delta\bar{S}^{xs}_{Fe}$
1.0	γ	1.000	1.000	0	0	0	0	0
0.9		0.903	1.003	-294	10	-21	0.188	-0.021
0.8		0.812	1.014	-602	41	-81	0.359	-0.084
0.7		0.724	1.034	-930	98	-196	0.506	-0.203
0.6		0.664	1.066	-1288	183	-380	0.627	-0.388
0.5		0.554	1.108	-1700	296	-667	0.713	-0.664
		(±0.014)	(±0.027)	(±70)	(±70)	(±400)	(±0.25)	(±0.25)
0.4		0.465	1.162	-2208	432	-1201	0.695	-1.126
0.3		0.373	1.242	-2845	623	-1975	0.600	1.792
0.2		0.271	1.356	-3760	877	-3108	0.450	-2.748
0.1		0.152	1.524	-5420	1215	-4678	0.512	-4.064
0.0	δ	0.000	1.778	$-\infty$	1659	-6779	∞	-5.819

REFERENCES

1. I. Langmuir, Phy. Rev. (2) 329 (1913).
2. M. Knudsen, "The Kinetic Theory of Gases" published by Meuthen ltd. London (1934).
3. P. Clausing, Ann. Phys. 12, 961 (1932).
4. R. Speiser and H. L. Johnston Tran. A. S. M. 43, 283 (1950).
5. K. Motzefeldt, J. Phys. Chem. 59, 139 (1955).
6. R. D. Freeman and A. W. Searcy, J. Am. Chem. Soc. 79, 5229 (1954).
7. R. D. Freeman and A. W. Searcy, J. Chem Phys. 23, 88 (1955).
8. W. K. Wilson, "Practical Solution of Torsional Vibration Problems" Pub. John Wiley and Sons N. Y. (1942).
9. J. J. Lingane and R. Karplus, Ind. Eng. Chem. Anal. Ed. 18. 3, 191-94 (1946).
10. R. Hultgren, R. L. Orr, P. D. Anderson and K. K. Kelley, "Selected Values of Thermodynamic Properties of Metals and Alloys". Pub. John Wiley and Sons, Inc. N.Y. (1963).
11. J. F. Butler, C. L. McCabe, and H. W. Paxton, Tran. A.I.M.E. 196, 221 (1961).
12. W. B. Kendall and R. Hultgren, Tran. A.S.M. 53, 199-205 (1961)
13. J. H. Smith, H. W. Paxton and C. L. McCabe, Tran. A.I.M.E. 221, 895-6 (1961).
14. A. P. Lyubimov, A. A. Granovskaya and L. E. Berenshtein Zhur. Fiz. Khim. 32, 1591-8 (1958).

15. C. Wells and R. F. Mehl, Tran. A.I.M.E. 145, 315 (1941).

16. R. A. Oriani and W. K. Murphy, Acta Met, 10, 879 (1962).

17. O. J. Kleppa, J. Phys. Radium, 23, 763-72 (1962).

18. R. J. Weiss and K. J. Tauer, Phys. Rev. 102(6) 1490-95 (1956)

19. C. T. Wei, C. H. Cheng and P. A. Beck, Phy. Rev. 112(3) 696-8 (1958).

20. R. J. Weiss and K. J. Tauer, Phys. Chem. Solid. 4, 135 (1958)

21. C. G. Shull "Theory of alloy phases", Pub. A.S.M. p. 279-89 (1956).

22. M. Hansen, "Constitution of Binary Alloys" Pub. McGraw-Hill Book Co. N. Y. (1958).

23. S. Dushman, "Scientific Foundations of Vacuum Technique", Pub. John Wiley and Sons, Inc. London (1955).

APPENDIX

The Knudsen equation for a finite hole thickness when the channeling effect is incorporated in the idealized equation is:

$$P_k = \frac{Z\sqrt{T/M}}{44.331 \times a \times t \times K_f}$$

where

P_k = P in atm.

Z = total weight loss in grams

T = T°K

M = Molecular weight of the vaporizing species

a = area of the orifice in cm^2

t = time of the experiment in seconds

K_f = Clausing correction factor obtained from Reference (24)

The correction factor C in Table VI is $\frac{K_f a \text{ (Experimental)}}{K_f a \text{ (Theoretical)}}$

K_f theorectical was obtained from the measured ratio of the hole radius (r) and the thickness (ℓ) using the table given in Reference (24)

TABLE VI

Calibration of Knudsen Cell with Pure Mn Sample

T°K	Wt. loss, gm.	Time, min.	P^{*}_{Mn}, 10^{-5} atm	Correction Factor, C	P^{**}_{Mn}, 10^{-5} atm	ΔH^{v}_{298}, cal
1273	0.1800	1400	3.18	0.9068	3.052	67148
1282	0.1890	1243	3.78	0.9068	3.626	67159
1358	0.4699	740	14.99	1.0062	15.90	66893
1388	0.7410	718	24.80	0.9752	25.58	66978
			Average	0.9478		
hole area ~ 0.0116 cm^2			$\frac{\ell}{r} = 0.9$	$K_f = 0.694$		
			$K_f \cdot a = 0.00805$ (Theoretical)			
1319	0.0858	1715	7.52	0.9621	7.455	67060
1321	0.0966	1865	7.79	0.9700	7.73	67080
1337	0.1094	1588	10.30	0.9779	10.34	67077
1379	0.1985	1407	21.40	0.9858	21.10	67046
			Average	0.974		
hole area ~ 0.0022 cm^2			$\frac{\ell}{r} = 1.6$	$K_f = 0.566$		
			$K_f \cdot a = 0.00125$ (Theoretical)			
1304	0.1339	1181	5.71	0.8585	5.684	67067
1311	0.2022	1523	6.49	0.8892	6.715	66971
1339	0.2632	1442	10.79	0.8585	10.79	67060
1350	0.2868	1163	13.06	0.8302	12.66	67141
			Average	0.8591		
hole area ~ 0.0077 cm^2			$\frac{\ell}{r} = 1.71$	$K_f = 0.550$		
			$K_f \cdot a = 0.00424$ (Theoretical)			

P^{*}_{Mn} Calculated from Reference (10)

P^{**}_{Mn} Recalculated using the average correction factor

TABLE VI (continued)

Manganese Vapor Pressure by Knudsen Effusion

x_{Mn}	Hole area cm^2	T°K	Wt. loss gms.	Time, min.	P 10^{-5} atm	$\Delta\bar{G}^{xs}_{Mn}$	a_{Mn}
0.0088	~0.0077	1310	0.0405	4200	0.4859	-396	0.076
		1349	0.0814	4200	0.9910	-359	0.077
		1393	0.1225	3000	2.122	-324	0.079
		1439	0.0890	1080	4.393	-321	0.08
	~0.01	1345	0.0755	2000	0.9210	-394	0.076
		1390	0.1237	1500	1.980	-370	0.077
		1440	0.1028	600	4.402	-331	0.079
0.347	~0.0022	1323	0.0743	4200	2.640	-164	0.326
		1359	0.0827	2500	5.003	-152	0.328
		1418	0.0855	1000	13.21	-137	0 331
	~0.0077	1345	0.0921	1200	3.919	-266	0.314
		1384	0.0881	600	7.605	-160	0.327
		1430	0.1083	360	15.84	-162	0.328
		1468	0.1052	200	28.06	-133	0.332
	~0.01	1368	0.1146	460	6.130	- 15	0.345
		1409	0.1050	230	11.40	-156	0.328
		1483	0.1551	122	32.57	-281	0.310
0.450	~0.0022	1325	0.0885	3600	3.672	-114	0.431
		1392	0.0753	1000	11.53	- 95	0.435
		1455	0.0704	360	30.61	- 79	0.440
	~0.0077	1331	0.1035	1280	4.107	- 96	0.434
		1482	0.1011	122	44.42	-153	0.428
0.546	~0.0022	1311	0.1000	4200	3.537	- 7	0.545
		1347	0.0903	2000	6.800	- 3	0.545
		1404	0.0758	660	17.66	+ 19	0.550
		1451	0.1030	442	36.42	+ 35	0.551
	~0.0077	1266	0.0942	3000	1.555	+ 29	0.550
		1333	0.1044	1000	5.318	- 10	0.544
		1439	0.1040	182	30.18	+ 14	0.549

TABLE VI (continued)

Manganese Vapor Pressure by Knudsen Effusion

x_{Mn}	Hole area cm^2	T° K	Wt. loss gms.	Time, min.	P 10^{-5} atm	$\Delta\bar{G}^{xs}_{Mn}$	a_{Mn}
0.597	~ 0.0022	1314	0.0802	2800	4.26	67	0.610
		1373	0.0700	890	11.96	107	0.618
		1453	0.0742	182	41.16	54	0.605
	~ 0.0077	1356	0.1183	700	8.664	14	0.597
		1394	0.0968	302	16.64	70	0.609
		1452	0.0943	122	41.01	91	0.613
0.699	~ 0.0022	1414	0.0375	210	27.54	125	0.731
		1440	0.0413	156	41.22	151	0.737
		1484	0.05735	116	78.14	132	0.734
	~ 0.0077	1332	0.05990	436	6.980	98	0.726
		1388	0.0672	186	18.74	128	0.734
		1421	0.0664	113	30.83	140	0.735
0.800	~ 0.0022	1312	0.1123	3100	5.38	40	0.813
		1382	0.1448	1200	18.41	62	0.819
	~ 0.0077	1336	0.1645	1000	8.375	39	0.813
		1405	0.1016	200	2.651	46	0.814

This report was prepared as an account of Government sponsored work. Neither the United States, nor the Commission, nor any person acting on behalf of the Commission:

A. Makes any warranty or representation, expressed or implied, with respect to the accuracy, completeness, or usefulness of the information contained in this report, or that the use of any information, apparatus, method, or process disclosed in this report may not infringe privately owned rights; or

B. Assumes any liabilities with respect to the use of, or for damages resulting from the use of any information, apparatus, method, or process disclosed in this report.

As used in the above, "person acting on behalf of the Commission" includes any employee or contractor of the Commission, or employee of such contractor, to the extent that such employee or contractor of the Commission, or employee of such contractor prepares, disseminates, or provides access to, any information pursuant to his employment or contract with the Commission, or his employment with such contractor.